

LAPPEENRANTA UNIVERSITY OF TECHNOLOGY

LUT School of Energy Systems

LUT Mechanical Engineering

*Iaroslava Andreeva*

**THE SUITABILITY OF COLOR LASER MARKING TECHNOLOGY INTO  
INDUSTRY**

Examiner(s): Professor Antti Salminen.

D. Sc.(Tech.) Hamid Roozbahani.

## **ABSTRACT**

Lappeenranta University of Technology  
LUT School of Energy Systems  
LUT Mechanical Engineering

Iaroslava Andreeva

### **The suitability of color laser marking technology for industry**

Master's thesis

2017

81 pages, 41 figures and 7 tables

Examiner(s):      Professor Antti Salminen  
                            D. Sc.(Tech.) Hamid Roozbahani

**Keywords:** Direct part marking, laser marking, color laser marking, colorimetry, wear resistance

In this thesis work, the technology of color laser marking of metals is considered from the point of view of its introduction into industry. The use of color images as a marking can provide not only product identification, but also attracts the attention of the consumers, and can also serve as an additional means of protecting products against counterfeiting. However, for industrial use it is necessary to standardize this technology and prove its compliance with the requirements of production. Thus, the goal is to test the technology of color laser marking for repeatability and resistance to various external influences. Therefore, a color palette for AISI 304 stainless steel consisting of fifteen colors was developed. The resulting colors were examined by optical, SEM and AFM, and the composition of oxide films was determined by Raman scattering spectroscopy. The standardization of colors and the repeatability of the palette were carried out by measuring and analyzing the reflectance spectra of the samples in accordance with the recommendation of the International Commission on Illumination. The stability of marking to the effect of various environmental conditions, mechanical and chemical effects is shown. Thus, possible limitations and recommendations for the introduction of technology in the industry were formulated.

## **ACKNOWLEDGMENT**

I would like to express my sincere gratitude to the LUT Laser and especially to Professor Antti Salminen for this great opportunity to conduct this research work. The work also would have been impossible without the immense support of my supervisor Hamid Roozbahani. I am really thankful to Ilkka Poutiainen for his support with the experimental setup and other technical issues.

I would also thank LUT Chemical engineering department for the help with the chemical resistance tests.

I also want to thank the Laboratory of Laser Micro- and Nanotechnologies of ITMO University in the person of Professor Vadim Veiko for the huge contribution to my professional development. I am extremely grateful to Russian researchers Galina Odintsova and Eduard Ageev for believing in me and their priceless pieces of advice during my studying in Finland and working at the thesis.

In addition, I am really thankful for help with the experiments to Saint Petersburg State University research park, especially to Alexander Shimko. Also I would like to acknowledge ITMO University Department of optical-electronic devices and systems, especially to Elena Gorbunova.

Iaroslava Andreeva

Lappeenranta 05.05.2017

## TABLE OF CONTEST

### ABSTRACT

### ACKNOWLEDGEMENTS

### SYMBOLS AND ABBREVIATIONS

<b>1</b>	<b>INTRODUCTION</b> . . . . .	<b>8</b>
1.1	Introduction to the laser based coloration . . . . .	9
1.2	Motivation behind the research and research problem . . . . .	10
1.3	Research questions . . . . .	10
1.4	Aim and objectives of the research . . . . .	11
1.5	Research methods . . . . .	12
<b>2</b>	<b>LITERATURE REVIEW OF METAL COLORATION TECHNOLOGIES</b> . . .	<b>13</b>
2.1	Conventional technologies of metal coloration . . . . .	13
2.1.1	Mechanical methods . . . . .	13
2.1.2	Chemical methods . . . . .	14
2.1.3	Thermal methods . . . . .	15
2.2	Laser methods of metal coloration . . . . .	16
<b>3</b>	<b>MATERIALS AND METHODS</b> . . . . .	<b>26</b>
3.1	Materials and the laser processing setup . . . . .	26
3.2	Spectrophotometry . . . . .	31
3.3	Color notation and calculations . . . . .	34
3.4	Other methods . . . . .	35
<b>4</b>	<b>OBTAINING OF COLOR PALETTE</b> . . . . .	<b>37</b>
4.1	Development of color palette . . . . .	37
4.2	Analysis of obtained structures . . . . .	45
<b>5</b>	<b>TESTING FOR REPETABILITY AND WEAR RESISTANCE OF COLORED SURFACE</b> . . . . .	<b>51</b>
5.1	Repeatability of obtained colors . . . . .	51
5.2	Environmental chamber test . . . . .	58
5.3	Mechanical resistance . . . . .	66
5.4	Chemical resistance . . . . .	68
<b>6</b>	<b>RESULTS AND CONCLUSION</b> . . . . .	<b>72</b>

<b>7 SCOPE OF FUTURE STUDY</b> . . . . .	<b>76</b>
<b>REFERENCES</b> . . . . .	<b>77</b>

## SYMBOLS AND ABBREVIATIONS

$a$	The material thermal diffusivity [ $m^2/s$ ]
$C$	Color
$d$	The distance between nearby grooves in the diffraction equation
$d_0$	Spot diameter at the focus point [ $\mu m$ ]
$d_i$	Mean of diagonals left by indenter [ $\mu m$ ]
$F_n$	Normal load [kg]
$f$	Laser pulse repetition rate [Hz]
$H$	Hatch distance [mm]
$I_0$	Power density (Intensity) [ $J/cm^{-2}$ ]
$J$	Maximum pulse energy [mJ]
$Nk$	Thermal conductivity [Wt/mK]
$L_x$	Overlap of laser spots along X-axes [%]
$L_y$	Overlap of laser spots along Y-axes [%]
$m$	An integer representing the propagation-mode of interest in the diffraction equation
$M^2$	Laser beam quality factor
$N_x$	Number of pulses per spot with the defined diameter along X-axes
$N_y$	Number of pulses per spot with the defined diameter along Y-axes
$P$	Laser power [W]
$P_{avg}$	Average power [W]
$P_{max}$	Maximum peak power [W]
$P_{nom}$	Nominal average output power [W]
$R$	Reflectivity
$R, G, B$	Red, green and blue components of flux used as a coordinates in CIE color space
$r, g, b$	Relative color coordinates in CIE RGB color space
$r', g', b'$	Primary colors according to CIE RGB system
$\bar{R}, \bar{G}, \bar{B}$	Units of the corresponding primary colors which should be taken to form
$S(\lambda)$	Radiant flux of light source

$T_0$	Initial temperature [°C]
$t_{eff}$	Effective time of laser action [ns]
$V_{sc}$	Scanning speed [mm/s]
$X, Y, Z$	Color coordinates in CIE XYZ color space
$x(\lambda), y(\lambda), z(\lambda)$	Color matching functions of the CIE LAB system
$\beta$	The angle of light diffraction
$\beta(\lambda)$	Spectral distribution of the reflection coefficient
$\lambda$	Wavelength [nm]
$\Delta E$ , delta E	Color difference according to CIE
$\Delta\lambda$	Emission bandwidth [nm]
$\Theta$	The angle formed by the grooves of the ripples in the diffraction equation
$\rho$	Reflection coefficient
$\rho_d$	Diffuse reflection coefficient
$\rho_r$	Specular reflection coefficient
$\tau$	Pulse duration [ns]
$\Phi_0$	Radiant flux of initial irradiation [W/m]
$\Phi$	Radiant flux reflected from the object [W/m]
$\Phi_{ob}(\lambda)$	Relative spectral distribution of the light source radiant flux reflected from the object [W/m]
$\Phi_s(\lambda)$	Spectral distribution of the radiant flux of the light source reflected from the reference white surface[W/m]
3D	Three-dimensional
AFM	Atomic force microscopy
CCD	Charge-coupled device
CIE	International commission on illumination
EDX	Energy-dispersive X-ray spectroscopy
LIPSS	Laser-induced periodic surface structure
LOMO	Leningrad Optical Mechanical Association
PVD	Powder vapor deposition
SAM	Scanning electron microscopy
XRD	X-ray Diffraction

## 1 INTRODUCTION

Marking of the products is one of the essential parts of production. Each item should have special symbol to identify product, give the information about manufacturer, properties or characteristics thus, ensure its quality. On the other hand, it has also emotional and motivational role due to impact of product labeling on the psycho-emotional state of consumers to meet aesthetic needs, as well as the motivation to buy. Thus, marks can serve to marketing purposes to attract the consumer's attention to the specific product.

Trade marking is the first information block that a consumer meets when choosing a product, and contains all the basic information. In this case, the marking of goods should be first of all clear and legible. In order to be visible mark should stand out or be placed on the background, contrasting with the color of the package (product). One more important thing is good resistance to climatic factors. Also, it should remain for the entire permitted period of use of the goods and be sufficient to ensure the safe handling of goods.

Usually in the structure of marking, three main elements can be distinguished: text, image or informative symbols. Depending on the use of product, its physical qualities, purpose and other factors, these elements could be used separately or together.

Text is the most common element, the most accessible to consumers and other subjects of market relations. In the text of the commodity marking, all forms of commodity information can be used. Images are applied to the goods to fulfill the emotional and motivational functions. It is the presence of a colorful pattern that facilitates the choice of goods by consumers. However, it is not always present on the labeling.

Information symbols are short and meaningful images bearing certain information. Many information signs can be deciphered only by specialists in the field of trade. Current information symbols are divided into the following groups: trademarks, appellations of origin, conformity or quality marks, bar codes, component signs, dimensional, operational, manipulative, precautionary, ecological etc.

Marks can be applied to products by different methods including removable such as labels, tags, control tapes, stamps or direct part marking. Last is the permanent marking methods



include variety of different techniques the main among them are indenting, coining, chemical and electrochemical etching, dot peen and also laser marking and laser peening. (Microscan Systems, Inc. 2017.)

Depending on number of factors among which are function of the product, geometry and size of a part to be marked, characteristics of surface including roughness and finishing methods, age life and the operating conditions.

Due to the number of advantages that lasers have laser marking is widely used nowadays in different areas of production to apply permanent, high resolution, contrast marks. This method is non-contact, rather fast, achievable to the different metallic or nonmetallic materials and does not require additional consumables or toxic solutions, thus, can reduce environmental pollution. Laser marking could be separated into engraving, laser etching, peening or annealing (color laser marking). Current work considers technology of color laser marking as the probably newest one and its applicability in industry.

### 1.1 Introduction to the laser based coloration

Effect of laser coloring of some metals has been known for a long time. Since 1980th this technology is being studied and many research groups are still interested in this topic. Usually, in scientific works questions related to possibility of use different kinds of laser sources, different environment and its effect on the result as well as overall analysis of physical and chemical properties are considering. This technology is related to the partial laser heating of the material to the specific temperature which results in formation of thin oxide film on the metal surface. Due to interference of light in this thin oxide layer and other optical effects it is possible to see the color. Depending on the thickness of the film these colors will be different. Thus, to obtain desired color oxide should have the determined thickness, that can be achieved by controlling the heating temperature and time of action. In turn, control of laser processing parameters allows monitoring the painting process.

Different types of laser, including  $CO_2$  lasers, UV lasers or solid state lasers can be used to achieve the result. Nowadays, the most popular for coloration and marking purposes are pulsed fiber lasers, due to the high flexibility, good optical characteristics, high productivity and relatively low cost of the equipment. Laser based marking tools are usually equipped with high speed scanning systems to control the move of laser beam on the surface with high accuracy.

Therefore, this method allows applying a colorful picture on different metals without using any dyes or chemicals. Technology is applied to the different oxidizable metals such as various alloys of steel, titanium, copper, brass, tungsten carbide and other.

### 1.2 Motivation behind the research and research problem

Color laser marking is very promising technology for industry. It can be used not only for normal marking, but for decoration of products and protection them against counterfeiting. On the one hand, this method as any of laser technologies, have high precision, flexibility, rather good productivity and number of another benefits. On the other hand, color laser marking technology has its own features and requirements, for instance the beam quality and stability of processing parameters.

Appearance and the rapid development of fiber lasers past years leaded to the rapid growth of laser marking international market (Shiner 2016, p. 82). Modern manufacturers prefer the use of laser technology as a reliable tool for marking their products. Thus, the thesis topic is relevant for modern production and interesting in order to introduce the new technologies to the market, Indeed, for industry it is very important to control the quality and repeatability of the production process. Each produced unit must be the same as a previous one and meets the standards of the factory. Therefore, the technology should be stable, repeatable and reliable to be implemented to the serial production.

The next question is related to of the product operating environment and age life of it. These factors are very important because they place limitations on methods which can or cannot be used in such conditions. It is subject to finishing of a product, possible methods of covering and of course to part marking.

Any technology if it is implemented to the industry, must be standardized, well described from the technological point of view (parameters are needed to reach the result, required equipment and equipment demands, material demands, required pre- and postprocessing etc.) and have specified working conditions. The research problem for this thesis can be formulated as the possibility of implementation color laser marking technology to industry and limitations of use.

### 1.3 Research questions

Color laser marking is widely investigated by many research groups from the scientific point of view. The questions about the oxidation mechanism, utilizing different laser sources as well as

analyzing of obtained structures and the influence of different experimental parameters. Mostly, all the researcher utilize pulsed fiber lasers for color marking but authors also discussed the possibility of use UV lasers (Li et al. 2009), CO<sub>2</sub> lasers. Also, there are a lot of works about analyzing of the grown oxide film, for instance in (Lawrence et al. 2013) the thickness of oxide film as well as its mechanical properties were shown. Chemical composition and structural analysis of obtained structures were throughly investigated in (Amara, Haïd & Noukaz 2015). The influence of gas environment where the process occurs is shown in (Luo et al. 2015).

Therefore, the process of color laser marking technology is rather good known and investigated. Moreover, some of using methods were patented. For instance, method of color marking a flat metallic part was proposed by Huf North American Automotive Parts Mfg. Corp. (Pat. US9205697B2 2014). Another methodology patented by Wroclawskie Centrum Badan Eit (Pat.EP2834034A1 2015). Authors also invented the system for color marking of metal.

However, for industrial implementation of color laser marking there are several issues that were not discussed yet. Thus, this thesis work have to give the answers for the following questions:

- (i) How laser processing parameters influence on produced colors and how to control them?
- (ii) How repeatable the results are?
- (iii) How resistant colors are?
- (iv) What are required parameters to the technology?
- (v) Are there any limitations of use the technology?

#### 1.4 Aim and objectives of the research

The main aim of this work is to prove the possibility of industrial implementation of laser color marking technology and develop the restrictions of its use. All the research questions are related exactly to the production, namely to technological process and terms of use the proposed method. To reach the aim it is necessary to fulfill the following specific objectives:

- (i) to describe the dependence of produced colors on the different laser processing parameters;
- (ii) to investigate obtained structures and to make a short analysis of relief, composition and other properties of the colors;
- (iii) to specify the colors and check the repeatability of them;
- (iv) to analyze the mechanical properties of the colors and make a conclusion about the mechanical resistance;
- (v) to check the colors for resistance to different environmental conditions;

- (vi) to discuss the chemical resistance of the colors to different solutions;
- (vii) to formulate the terms of use the technology and to specify any possible limitations;
- (viii) make conclusion about the suitability of color laser marking technology for industry.

### 1.5 Research methods

Laser color marking technology can be implemented in LUT Laser with the use of experimental setup based on ytterbium pulsed fiber laser equipped with two-axis beam scanning system. Stainless steel AISI 304 was under the study of this thesis.

First of all, the development of color palette for further examination was required. To make the wide color range it was necessary to change almost the all parameters of laser source as well as scanning system parameters. Thus, first step was to achieve the clear dependence of color on each processing parameter. In order to achieve this, matrixes of colors were produced changing two parameters at the same time and fixing the other parameters. From each matrix, the most successful colors were chosen. The next stage was separation the stable colors by testing each regime with the different sizes of image and place within the marking field.

After development of color palette, the analyze of the treated surface was required. To study the structure of obtained oxides methods of optical and scanning electron microscopy (SEM) were used. To examine the obtained relief the AFM (atomic force microscopy) in the contact mode was utilized. By Raman spectroscopy the chemical composition of oxide films was found.

After the examination of obtained structure the repeatability of the color palette was proved. The reflectance spectra were measured for each color. Then the method of calculation the color dependence was performed according to the standard algorithm providing by International commission on Illumination (CIE).

Last stage was proving the mechanical and chemical resistance of colors. To determine the mechanical resistance hardness of obtained colors was compared to the hardness of initial material. To estimate the chemical resistance the reaction of obtained color palettes to the different chemical agents was observe. Results were analyzed visually and under the optical microscope as well.

## 2 LITERATURE REVIEW OF METAL COLORATION TECHNOLOGIES

In this chapter the comparison between the conventional technologies of metal coloration and color marking with the technology of color laser marking is presented. Color laser marking can be realized by many different ways, with the use of different lasers and implementing various gaseous environment. All the main ideas of color laser marking are explained in detail.

### 2.1 Conventional technologies of metal coloration

In the current work the formation of thin oxide films on the stainless steel surface due to nanosecond pulsed laser exposure is introduced. When metals are heated below the evaporation temperature, thin oxide films form on their surfaces. As a result of the interference in this oxide layer colors may appear. Depending on the thickness and light incident angle the color will be different. This effect can be applied both in decorating products, and in creating unique signs that protect products from counterfeiting.

Apart from the laser oxidation there are many conventional technologies which can be used to produce colorful covers and identification symbols on metals. Among them there are mechanical coloring, chemical and electrochemical thermal methods.

#### 2.1.1 Mechanical methods

In general, there are several ways to color metallic products:

- (i) Powder painting. The essence of this method is that electrically charged particles of paint in powder phase are sprayed onto the precleaned product. The product to be painted has an opposite charge. After that, the product is "baked" in the polymerization chamber (Misev & Van der Linde 1998, pp. 163-165);
- (ii) Tapping of coloring powders , i.e. tapping of colored wires or metal plates into etched grooves on the product;
- (iii) Application of enamels;
- (iv) Physical vapor deposition (PVD)

PVD method is related to vacuum deposition of atoms or molecules of desired material. The deposited material from the solid or liquid phase is converted into a gas state and, passing through a vacuum or low pressure atmosphere, precipitates on the surface of the material being processed. Typically, vacuum deposition is used to deposit films with a thickness of from one

to a thousand nanometers. However, this technology can be used for building of solid structures by multi-layer deposition. The deposition rate of the film depends on many factors, but usually varies within 1-10 nm per second. (Bouzakis & Michailidis 2014.)

Thus, in work (Panjan et al. 2014) it was proposed to use this technology for decorative applications, namely for the creation of stable color coatings. Due to interference effects on translucent and reflective surfaces and variation in thickness of deposited films, the possibility of coloring materials in different colors was demonstrated. Films were deposited on silicon, glass and metal substrates. The process of sputtering consisted of three main stages. The first stage was the formation of a protective coating of AlTiN / TiN with a thickness of 3  $\mu\text{m}$ . The next step was the deposition of a reflective coating with a thickness of 80 nm (TiN) and a translucent 50 nm coating (AlTiN). In this case, a reflective coating and a translucent coating were imparted to a dark blue color of the material. Also, one of the necessary stage of the process is additional heating of the substrate to the temperature of about 450 °C. The concrete color was adjusted by varying of film thickness in the range of 25-55 nm that corresponded to yellow, pink, purple and blue shades (Panjan et al. 2014, p. 68).

Indeed, regarding to the stability of the films being formed, layers with a high Al content can be referred to as stable, which is based on a high hardness and high resistance to oxidation at high temperatures. It can also be said that the AlTiN coating is distinguished for its excellent mechanical and significant optical properties, which can be used to create coatings with protective and decorative functions. Among the disadvantages of this technology are that the process includes several operations, thus it is time consuming, and pictures with the different shape and colors cannot be produced. The main advantage of the technology is the possibility of coating very complex shapes with a good uniformity.

### 2.1.2 Chemical methods

Chemical staining involves the modification of the metal surface by the formation of chemical compounds on the surface (thin interference oxide or nitride films) or galvanic depositions. Therefore, the metallic surface takes color, but the properties of the material itself do not change. Chemical coloring can also be accomplished applying an electric current (metallochromy). One of chemical coating methods is the chemical development of thin interference film on the surface. The principle involves application of hot solution of sulfuric acid with the dispersed ions of chromic acid salts (Burns & Bradley 1967). The electrochemical methods or anodizing

mean the process of obtaining oxides on the of metal surface during anodic polarization in oxygen-containing solutions with ionic conductivity. Usually anodizing is carried out on a direct current in galvanostatic or controlled potential electrolysis. Depending on the type of oxygen-containing media that fills in the interelectrode space, anodizing can be implemented in aqueous solutions of electrolytes, in salt solutions, in plasma gas. (Blawert et al. 2006.)

When anodizing in a plasma gas, oxides form due to mutual diffusion of metal cations and oxygen anions from the plasma. With other types of anodizing, the oxide is an electronically oriented polymerized metal oxide gel. Nonthermal plasma, which is formed in the immediate vicinity of the metal surface under the oxide, is the source of oxygen anions necessary for the formation of oxide.

For example, in (Blower & Evans 1974, p. 232) anodizing is carried out by applying an alternating current to a material located in a hot solution of sulfuric acid. The chemical oxidation of the stainless steel surface in a sulfuric acid solution was carried out by a similar method, but at the ambient temperature (Ogura, Sakurai & Uehara 1994, p. 649). However, the stability of the oxides obtained by these methods proved to be extremely low to the common mechanical cleaning methods are used in real production.

Another method of electrochemical coloring, based on the influence of a pulsed electrical current, allows one to obtain oxide coatings that are more stable to the external effects. Authors of (Junqueira & de Oliveira Loureiro 1984, p. 43) investigated samples of four colors: brown, blue, gold and green. By using method of spark atomic emission spectroscopy, the thicknesses of the produced films were determined respectively brown -70 nm, blue -130 nm, gold -300 nm and green -440 nm. Testing the samples for hardness and resistance to mechanical friction showed that thicker films, corresponding to gold and green colors, are softer but more resistant to the abrasion.

### 2.1.3 Thermal methods

In addition to mechanical, chemical and electrochemical methods of coloration, the creation of interference oxide films by the thermal method is also included to the conventional technologies. The essence of the technology of thermal coloration is the formation of interference films (tampering colors) on the surface of the material when it is heated, for example, in a furnace. Colors form corresponding to the heating temperature and exposure time. In (Birks, Meier &

Pettit 2006, p. 102) the dependence on the temperature is shown for stainless steel samples annealed in a furnace: a light yellow color corresponds to 220-240 °C, an orange color: 240-260 °C, a red-violet: 260-280 °C, blue: 280-300 °C.

In general, the aforementioned technologies and methods have their advantages such as low cost and wide color palette (mechanical), relatively good wear resistance (PVD, electrochemical and thermal coloration). However, each of these methods have also limitations and disadvantages. (Pat. US4869789A 1989.)

In case of mechanical coloration, there is a need to use consumables (paints, enamels, wires, chemicals, etc.). They are also could be time-consuming and labor-intensive, since they require an additional stage - preliminary preparation of the products (degreasing, cleaning or preheating of the product surfaces).

In case of PVD, the extremely low productivity of this technology makes it difficult to industrial implementation. At the same time, these methods do not allow to obtain images with high resolution. On the other hand, chemical and electrochemical methods can provide only a limited palette of colors. Also, the inability to apply more than one color in one cycle, the need for consumables (electrolyte solutions) that have a negative effect on environment, and the complexity of controlling the process of creating the concrete color coating, can cause new restrictions in the utilizing of the methods. Coatings created by powder painting and some chemical methods have low resistance to mechanical action.

## 2.2 Laser methods of metal coloration

Laser oxidation of metals provides ample opportunities for creating color images with high resolution on oxidize metals. At this point there are large number of studies related to the laser oxidation of the metal surface for its coloration. Investigations in this field have been actively pursued for the last fifteen years, and to date it is known about the possibility of coloring the metal surface by forming thin oxide interference films with Nd:YAG, CO<sub>2</sub> fiber and excimer lasers (Pat. US6238847B1 2001). Also, there is a method of laser coloration by formation of diffraction structures on its surface with ultrashort laser pulses (Dusser et al. 2010).

One of the possible methods of creation oxide films is related to the use of excimer lasers and been investigated by several research groups. For instance, in (Jervis et al. 1990), the creation of oxide films on the surface of AISI 304 steel plates in air was presented using an excimer



laser with the wavelength of  $\lambda = 248 \text{ nm}$  and a pulse duration of  $\tau = 25 \text{ ns}$  an overlap of 80 %. According to the results, it was proved that the energy density of  $1 \text{ J/cm}^2$  is sufficient to produce gold or yellow colors on the surface. The dependence of the thickness of the growing film on the number of laser pulses arriving at one point on the surface has a linear form. The composition of the obtained oxides can be written as  $A_3B_4$ , where  $A = (\text{Fe}, \text{Cr}, \text{Ni})$  and  $B = (\text{O}, \text{C}, \text{N})$ . In this case it is taken in assumption that C and N replace O at lattice sites.

Also, other short wavelengths lasers have been proposed to use for metal coloration purposes. In (Li et al. 2009) authors studied the oxidation of the AISI 304 steel in order to obtain various colors on its surface using the third harmonic of the radiation of an  $Nd : YVO_4$  laser. The emission parameters were following: wavelength of  $\lambda=355 \text{ nm}$ , pulse duration  $\tau=25 \text{ ns}$ , spot diameter at the focus point of  $d_0 = 13 \text{ mm}$ , average power  $P = 7\text{-}10 \text{ W}$  and pulse repetition rate was  $f = 40 \text{ kHz}$ . Among the parameters which affected on the resulting color authors determined such parameters as the radiation power, the defocus amount of the beam (these two parameters can be combined in power density) and the scanning speed.

The initial oxidation reaction depends on the scanning speed of the laser beam. At the speed of about  $500 \text{ mm/s}$ , only those areas of the surface where the chromium concentration is higher can be oxidized, thus, clusters of  $Cr_2O_3$  oxide are formed. At the scanning speed of  $400 \text{ mm/s}$  a uniform a two-layer oxide structure is formed. The composition of this two-layer film was investigated and it was determined that the film is consist on chromium oxide  $Cr_2O_3$  (thick lower layer) and the iron oxide  $Fe_2O_3$  (upper thin transparent layer). (Li et al. 2009, p. 1584.)

The thickness of the growing oxide increases due to diffusion of iron to the surface, and the presence of chromium in the oxide film decreases with the increasing of the number of passes. The growth rate of the oxide film decreases with the number of passes, and the thickness of this film tends to become established. This phenomenon occurs because the thickness of oxide film becomes too large and the average amount of microcracks on the oxide surface increases, that is restrict the distribution of O atoms throw oxide layer and its reaction with Fe atoms of the material. (Li et al. 2009, p. 1585.)

Nowadays, it tends of extinction in the usage of fiber lasers in the different fields of production and processing. These lasers can be easily implemented in a production line, because its flexibility, they have good lateral distribution of the beam, thus, high quality of it and number

of other advantages. Therefore, this type of lasers is widely used for engraving and marking, including color marking of metals. There are huge number of research groups who utilize fiber lasers for the coloration purposes.

The possibility of creating interference oxide films on the surface of 304L stainless steel was demonstrated in (Adams et al. 2013). For the research authors used the radiation of a nanosecond fiber laser with the wavelength of 1064 nm. Pulse duration was 120 ns, spot diameter of the beam focused right on the surface was 59  $\mu\text{m}$ , and the energy density varied between 600 to 800  $\text{J}/\text{cm}^2$ .

The results of SEM (scanning electron microscopy) given in the work showed that the thicknesses of the oxide films formed in the study were in the range of 20-500 nm. Figure 1a shows the reflection spectra of samples obtained at scanning speeds of 500-600 mm/s. The thicknesses of these films were within limit of  $\frac{1}{4}$  of the wavelength of the incident radiation. In this case, interference effects do not affect on the color of the surface. Figure 1b shows the reflection spectra of samples obtained at scanning speeds of  $100 \pm 450$  mm/s. Here the thicknesses of the produced films were  $341 \pm 31$ ,  $285 \pm 31$ ,  $100 \pm 11$ ,  $65 \pm 6$  nm, corresponding to an increase of scanning speed. For this films, interference plays an important role in resulting colors of the surface. (Adams et al. 2013, pp. 3-5.)

XRD (X-ray diffraction) spectra showed that the composition of thin oxide films (up to 250 nm) is  $\text{MnCr}_2\text{O}_4$  and/or  $\text{Fe}_3\text{O}_4$  (Adams et al. 2013, p. 5). Indeed, thicker films ( $> 250$  nm) have the same composition as it was shown in (Li et al. 2009). Therefore, they are the bilayer structures, where the upper layer is iron oxide, and the lower one is chromium oxide. Also, it was presented that the growth of oxides due to laser action significantly changes the composition and structure of the metal surface. The occurrence of oxides reduces the concentration of chromium in the substrate. The depth of this degenerate state is almost equal to the thickness of the oxide film. The layers of laser-modified material close to the surface turn from the austenite phase to ferrite.

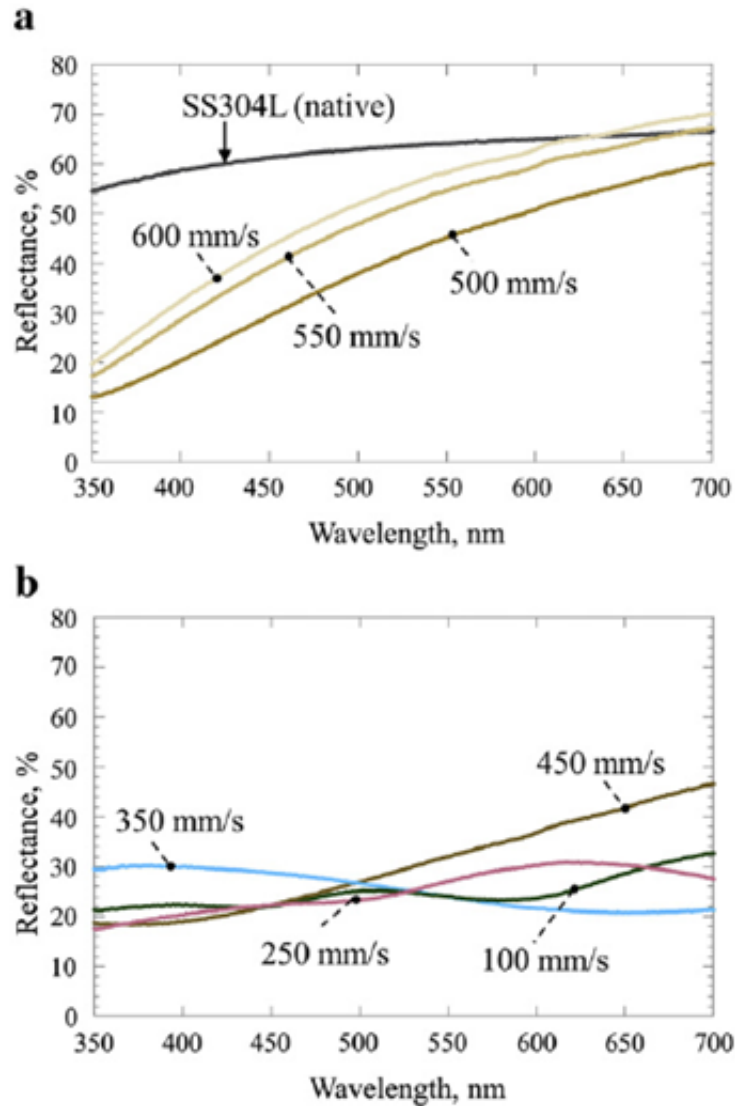


**Figure 1.** Reflectance spectra of obtained colors: bare SS 304L and three thin metal oxide coatings made using average power  $P_{avg}=5.6$  W and scan speeds of 600, 550 and 500 mm/s - (a); oxide coatings made using  $P_{avg}=5.6$  W and scan speeds of 450, 350, 250 and 100 mm/s - (b). (Adams et al. 2013, p. 7.)

Next study (Luo et al. 2015) shows how the different gas environment in which the sample is located during the laser action influences to the composition and color of the modified surface.

Polished stainless steel plates were cleaned with acetone and deionized water. After that, they were placed in a special chamber. The window could pass 90% of laser radiation with a wavelength of 1064 nm. The chamber was filled with one of the gases (air,  $O_2$ ,  $N_2$ , Ar) and authors compared the results of processing with the same parameters under the different gas conditions. Samples obtained after irradiation in different environment by laser radiation with

a pulse duration of 10 ns and a repetition rate of 35 kHz are shown in figure 2.

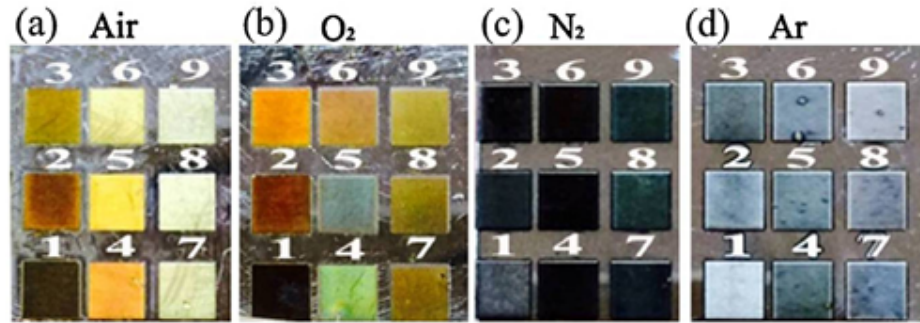


**Figure 2.** Influence of gaseous environment on the produced colors obtained on stainless steel with the laser scanning speed varied from 10, 20, 30, 40, 50,60, 70, 80 to 90 mm/s (Luo et al. 2015, p. 406).

The relief of microstructures formed by laser pulsed action on the surface of stainless steel, according to the authors, strongly depends on the scanning speed (fig. 3). Oxygen-rich environment accelerate the growth of nanostructures formed during laser exposure. When oxidizing in air, "branched" nanostructures are formed. Similar structures, but of a larger size, are formed when oxidizing occurs in  $O_2$ , whereas in  $N_2$  and Ar their growth is markedly suppressed and separate nanoparticles are formed on the surface. Elemental analysis showed that the chemical composition of the modified surface is particularly affected by the laser exposure parameters. (Luo et al. 2015, p. 407.)

During the oxidation in air and in  $O_2$  environment, the concentration of the oxygen in the material gradually decreases, while the concentration of Fe, on the contrary, increases with the increasing scanning speed. In oxides obtained in  $N_2$  and Ar environment, the concentration of O is lower than 13%, and the concentration of Fe is higher than 42%. The more oxygen is involved in the process of the laser oxidation of metal samples, the more friable the oxide structure is formed and the more intense the color appears. The maximum oxygen concentration on the modified material corresponds to a scanning speed of 50mm/s. (Luo et al. 2015, p. 408.)

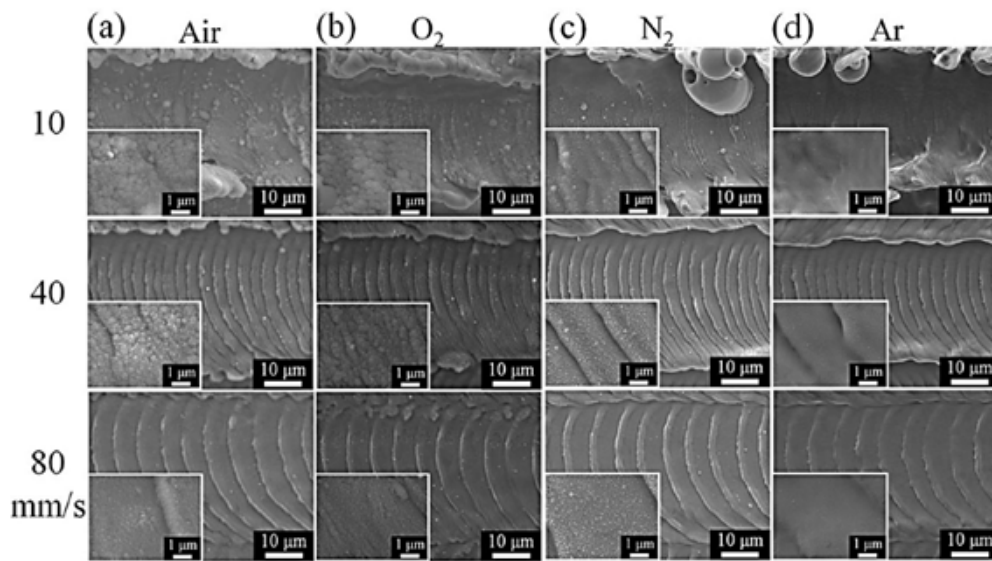


**Figure 3.** Type of surface structures obtained on stainless steel in different gaseous environments at scanning speeds of 10, 40 and 80  $mm/s$ " (Luo et al. 2015, p. 407).

One of the laser methods of material coloration which can be used not only for metals but also for semiconductors is the formation of diffraction nanostructures on its surface by the action of ultrashort pulses. Several mechanisms for creation of this kind of structures were considered by many authors. One of the most fundamental one is (Dusser et al. 2010), where authors perform analysis of obtained structures and shows dependence of produced colors on the laser processing parameters. The effect of coloring the surface is achieved by diffraction of light on periodically located specially oriented nanostructures created by the action of a Ti:Sa laser radiation with a pulse duration of 150  $fs$ , the wavelength of 800  $nm$  and the repetition rate of 5  $kHz$ . These nanostructures, whose size is noticeably smaller than the wavelength of the radiation and the wavelengths of the visible range, are called LIPSS (Laser-induced periodic surface structure) or ripples. This effect occurs due to the interference of incident femtosecond laser radiation acting on the surface of the material and scattered or excited surface waves.

In the first place, authors have studied the influence of polarization of laser radiation on the ripples orientation. The process of interaction consists of the absorption of the laser pulse energy and its distribution in the material. The energy distribution and the effects associated with it are established by the relaxation time. In other words, for this short interaction the time of laser action is not enough for material to conduct the heat. The energy cannot be distributed directly through the conductivity of the material, but it excites the free electrons first and then

electrons relaxes, thereby, distribute the energy to the crystal lattice so heat the material after the end of the laser pulse. (Dusser et al. 2010, pp. 2915-2917.)

As a result of the thermodynamic phase transition, a local modification can take place on the surface of the sample, the form of which will depend on the power density of the laser pulse. The formation of nanostructures occurs for energies near the ablation threshold. The surface undergoes local melting followed by re-solidification, thus, long periodic structures can form. With the exceeding of the ablation threshold, it is difficult to obtain continuous structures because of partial screening of the radiation and the destruction of previously formed structures due to extra heat input. (Dusser et al. 2010, p. 2918.)

In the article the ripples of different orientation and the period were obtained on the stainless steel with the linearly polarized femtosecond laser radiation. The concrete color in this case is related to diffraction effects, namely they depend on the period of produced diffraction grating and the incident angle. The wavelengths corresponding to the different colors resulting from the obtained ripple orientation are calculated using the diffraction equation (Dusser et al. 2010, p. 2919):

$$m\lambda = d(\sin \alpha \cos \Theta + \cos \beta) \quad (1)$$

where  $\lambda$  is wavelength,  $d$  is the distance between nearby grooves,  $m$  - an integer representing the propagation-mode of interest,  $\alpha$  is the angle of incidence of light,  $\Theta$  is the angle formed by the grooves of the ripples,  $\beta$  is the angle of light diffraction.

Therefore, a full color palette (fig. 4) was obtained under different laser processing parameters, depending on the number of pulses arriving at one point on the surface ( $N_b$  (p)) and the polarization angle, thus with the different ripple orientation angles in the range of  $0^\circ - 90^\circ$ . Thus, authors have illustrated the method of coloring the surface based on the theory that one orientation of the ripples corresponds to one color.

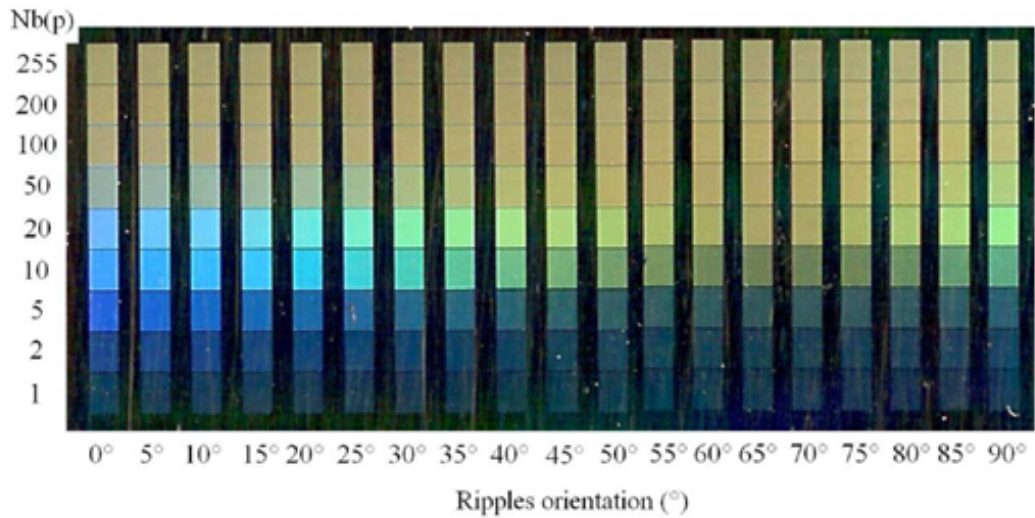


**Figure 4.** According to (Dusser et al. 2010, p. 2920): "Scanned image (1200 dpi) of stainless steel sample (316L) marked by 9 lines of nineteen squares obtained with the “optical way 1” femtosecond laser chain (Power,  $P = 25 \text{ mW}$ , power density  $I_0 = 0.4 \text{ J/cm}^{-2}$ ). Each line uses a “point by point” marking method and each square has been marked with different ripples orientations (from  $0^\circ$  to  $90^\circ$ ). Each point of the scroll up lines has been marked with different numbers of laser pulses (from 1 laser pulse/point on the bottom line to 255 laser pulses/point on the top line)".

The productivity of this method is rather high: authors approved that to produce one picture of  $15 \times 15 \text{ mm}$  size, having at least 6 different colors, generally 3 minutes is enough. But this time can be reduced by adjusting of the processing parameters, such as scanning speed, repetition rate etc. (Dusser et al. 2010, p. 2922.)

But utilizing pico- and femtosecond lasers in the serial production have many restrictions due to high equipment cost, expensive and complex maintenance of the equipment, low flexibility and high operational requirement. Thus, this method still has not find many industrial applications.

On the other hand, fiber lasers with nanosecond pulse length have many advantages over all listed laser instruments for coloring metals. Specifically, they provide high reproducibility of results due to stability of laser beam and high accuracy of setting the parameters. They are also convenient to use, relatively inexpensive (in comparison with lasers of ultrashort pulses) and compact, that is undoubtedly important in industrial applications.

The other question is how to find right parameters of laser processing, that will be productive and

stable at the same time. Efficient method of development of colors on stainless steel by recording and analyzing of the spectrophotometric characteristics of obtained colors was proposed in Veiko et al. (2016). The idea of this technique is to make experimentally at least five basic colors on the material. Then authors measured the reflectance spectra (fig. 5a) of them and calculated the color coordinates. The full color palette can be found by analyzing the displacement of the reflectance spectra depending on the laser processing parameters (fig. 5b). Therefore, having only five experimental colors, the full possible color palette can be found theoretically. Thus, the time of preparation can be significantly reduced, which is very important in real production process.

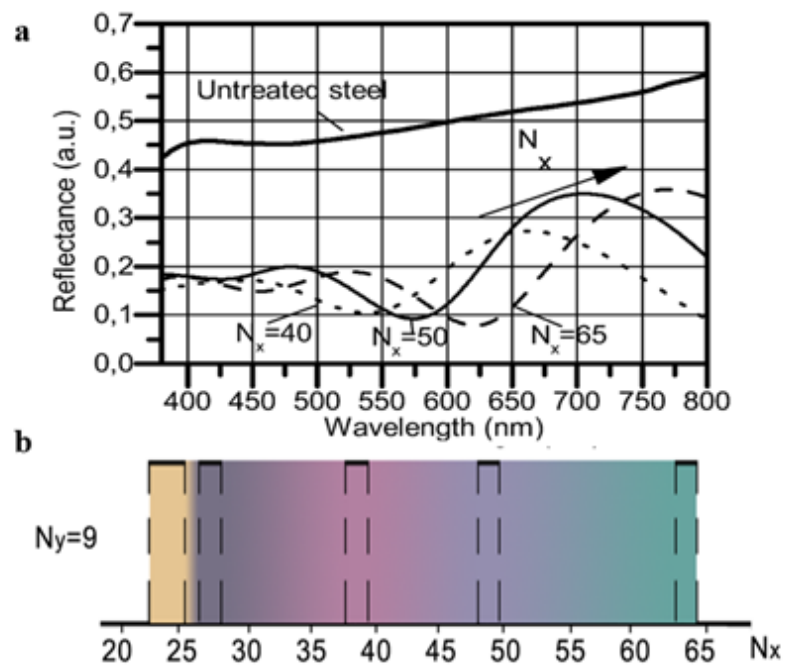


**Figure 5.** Colors obtained for  $I_0 = 2.9110^7 \text{ W/cm}^2$ ,  $N_y=9$ : reflectance spectra before and after laser treatment corresponding to interference colors (a); complete color palette. The dashed lines correspond to colors obtained experimentally (b). (Modified (Veiko et al. 2016, pp. 686.)

Authors proved that the colorimetric characteristics for interference colors unambiguously depend on the processing parameters and it can be defined for concrete material and used for the development of new colors (Veiko et al. 2016, pp. 687).

Summarize the results, fiber lasers of nanosecond pulse length can be identified as the most promising instrument for color laser marking. On the one hand, it has many benefits over conventional metal coloring methods as well as other the rest of laser technologies. On the other hand, there are large number of research groups who have successfully investigated the main



characteristics and features of this method.

However, for production there are some special mandatory requirements related to the quality of the mark. These requirements can be divided into two classes: the first one is repeatability and reliability of obtained colors and the second one is the sustainability of them. Following work will present the analyze of possibility of implementation the color laser marking technology in industry.

### 3 MATERIALS AND METHODS

This chapter is describing the motivation behind choosing the materials which are used in the thesis, its properties and means of preparation, description of the experimental setup and also methods of examination of obtained samples.

#### 3.1 Materials and the laser processing setup

Different alloys of stainless steel are widely used in many areas of modern production, such as heavy engineering, the production of electronics, precision mechanics and household appliances, in construction and architecture, electric power, pulp and paper production, food, chemical and petrochemical industries, transport engineering, etc. The presence of chromium in the composition of stainless steel gives the alloy high heat resistance and chemical stability. In the current work stainless steel AISI 304 2 mm thick plates are used. The important for laser interaction characteristics of the material are presented in table 1. AISI 304 is austenitic Cr-Ni stainless steel consist of 71% Fe, 0,08% C, 18% Cr, 10% Ni and small amount (less than 2%) of other alloy additives – Mn; Ti, Si, S, P, Cu, Mo, W, V (Baddoo & Burgan 2001, p. 18). Samples was cleaned with acetone before treatment to avoid a dirt or fingerprints.

*Table 1. Physical and optical properties of AISI 304 stainless steel (Baddoo & Burgan 2001, p. 30).*

Property	Unit	Value
Reflectance R ( $\lambda = 1.06 \mu m$ )	-	0.75
Thermal diffusivity a	$10^{-6} m^2/s$	3.00
Thermal conductivity k	$W/mK$	37.00
Melting point	$^{\circ}C$	1800
Boiling point	$^{\circ}C$	3145

The experimental setup, the visual appearance of which is shown in fig. 6, was assembled by means of LUT Laser laboratory. As it was proved previously, fiber lasers have all the necessary parameters for laser color marking, as well as the material provides rather good adsorption for near infrared wavelength range. Therefore, commercially available ytterbium fiber laser with nanosecond pulses produced by IPG Photonics corporation was chosen as the source of laser radiation. The main characteristics of laser is performed in table 2. It is diode pumped pulsed laser with the random polarization of output radiation. This source provides average power of 20W and have good beam quality ( $M^2 < 2$ ) and Gaussian beam profile.

Table 2. Main optical characteristics of the laser source (modified IPG Photonics Corp. 2017).

Characteristic	Unit	Value		
		Min	Typical	Max
Pulse duration, $\tau$	ns	4, 8, 14, 20, 30, 50, 100, 200		
Central emission wavelength, $\lambda$	nm	1055	1064	1075
Emission bandwidth, $\Delta\lambda$	nm		5	10
Nominal average output power, $P_{nom}$	W	19	20	21
Output power adjustment range	%	10		100
Extended pulse repetition rate, $f$	kHz	1.6		1000
Maximum pulse energy, J	mJ		1	
Maximum peak power, $P_{max}$	kW		15	

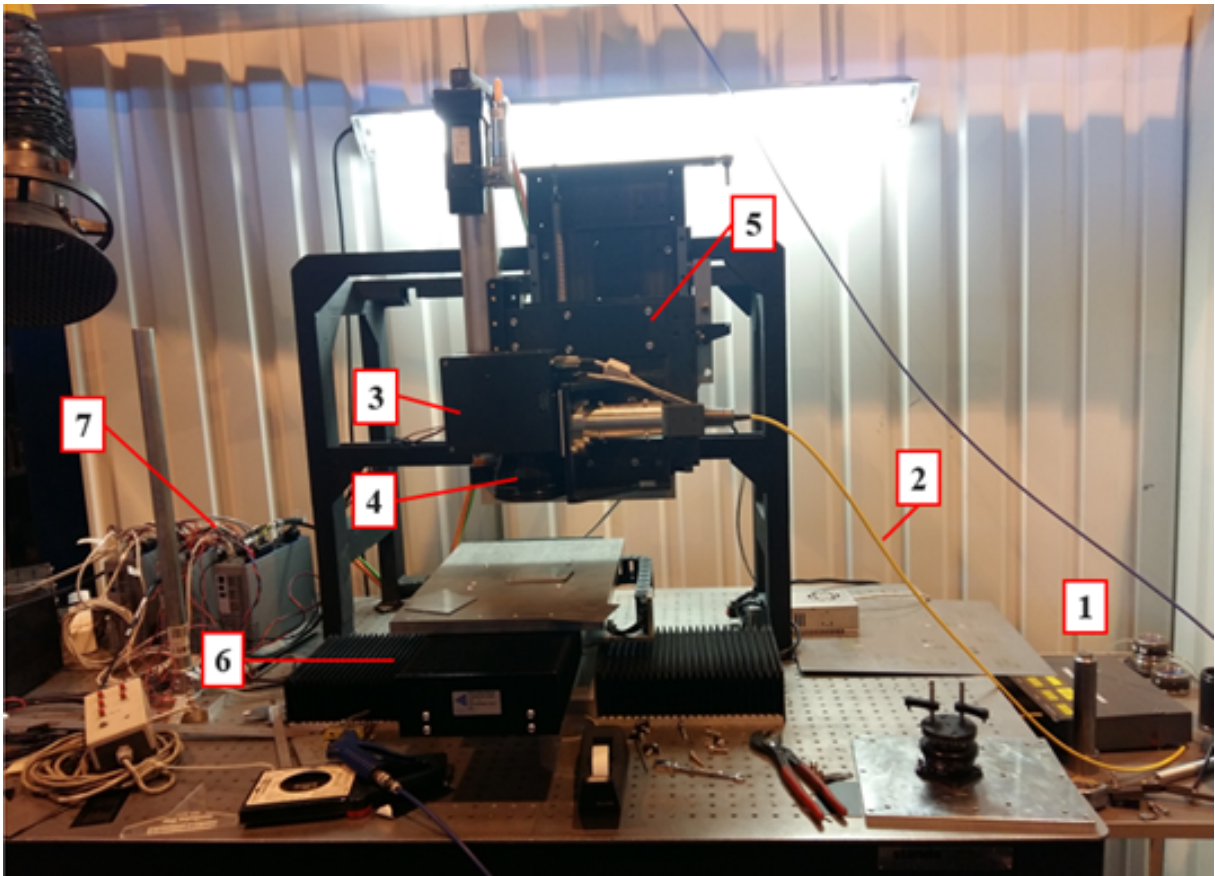


**Figure 6.** Laser marking system based on nanosecond fiber laser: 1 – nanosecond fiber laser from IPG Photonics; 2 – delivering optical fiber, 3 – scan system from SCANLAB, 4 – 100 mm lens; 5 - linear actuator for vertical movement from Neff-Wiesel; 6 – XY coordinate stage, 7 – ACD servo drives from Kollmorgen.

Laser-induced action was done according to the schematic diagram shown in figure 9. The

radiation of a fiber pulsed ytterbium laser (1) along an optical fiber (2) was fed into a collimating system (3), which forms an output parallel beam. A two-axis galvanometric scan system (hurry SCAN II 14 digital scan head from SCANLAB corp.) consisting of two mirrors (4) and (5), provided the laser beam was moved along the X and Y axes. Scan head system and laser are synchronized with the RTC4 interface board integrated in PC. After the scanning system, the radiation was focused by an objective (6) with a focal length of 100 mm on the surface of the steel plate (7). Vertical movements is carried out with the ball screw linear actuator from Neff-Wiesel. Also, the additional horizontal movements can be done with the multiaxial linear motor coordinate stage (8) that can extend the work field up to 250x250 mm. Kollmorgen AKD servo drives (9) and Real-Time PXI controller PXIe-1071 from National Instruments (10) are used to control the motions of XY-stage and Z-axis. Due to logical encoder it is possible to move the sample with rather high accuracy of about Controlling and synchronization of all the components is carried out from PC (11). LAB View code, developed in the LUT Laser, allows to change the parameters of radiation, scan speed, as well as manage any vertical and horizontal movements.

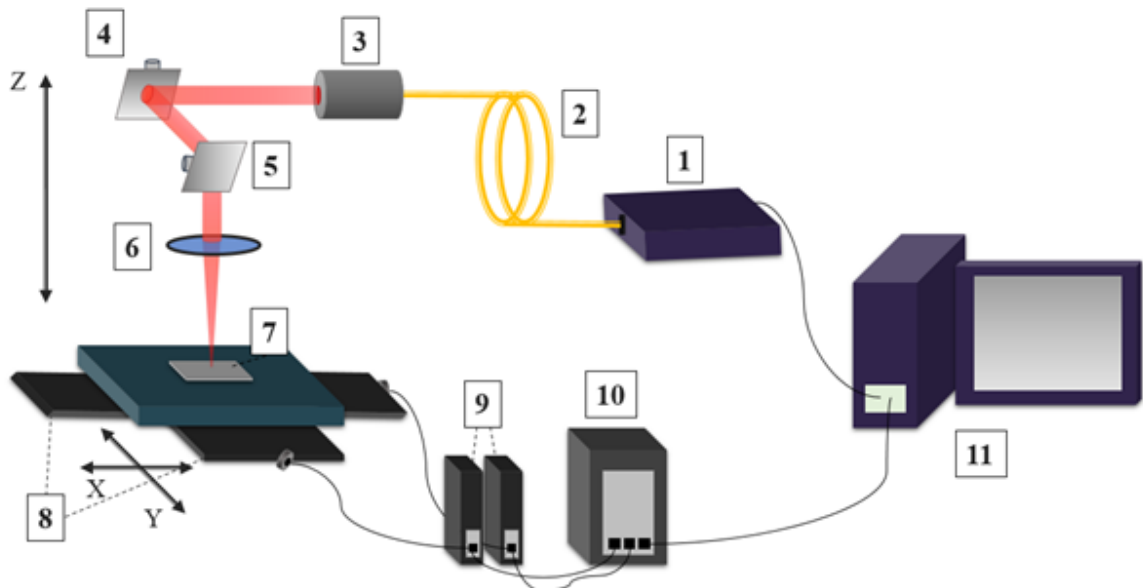


**Figure 7.** Schematic diagram of the experimental setup, where 1 – fiber laser, 2 - transferring optic fiber, 3 – collimator, 4, 5 – scan head mirrors, 6 – focusing lens, 7 – sample, 8 – two axial movement stage, 9 – drivers, 10 – controller, 11 – PC.

Scanning of the surface of the samples was carried out as it shown on the beam scanning scheme in fig. 8. The surface is irradiated by line-by-line scanning of a focused laser beam with a

diameter  $d_0$  moving at a velocity  $V_{sc}$ . After passing one scan line with the repetition rate of laser pulses in beam f with defined overlap of  $L_x$ , (%) the beam moves along the axis Y on the next line according to the overlap  $L_y$  (%) defined by hatch distance H. The overlap is also can be defined with the number of pulses for one spot with a diameter  $d_0$ :  $N_x$  and  $N_y$  along the axis X and Y correspondingly.

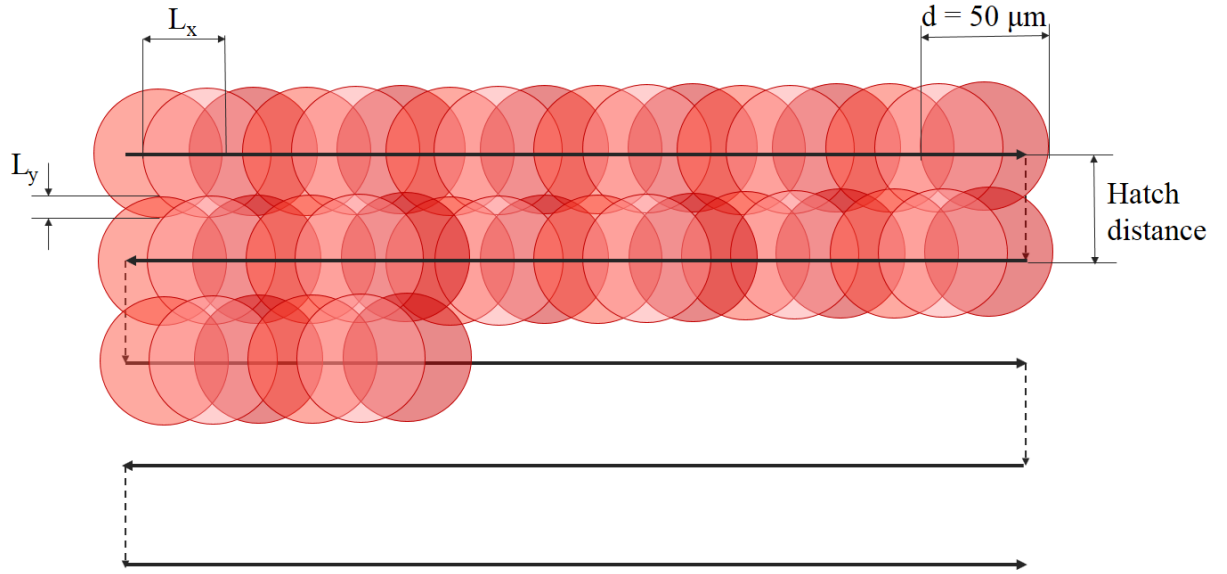


**Figure 8.** Scheme of laser scanning.

In general, color depends on the thickness of obtained film. Different thicknesses can be produced by adjusting laser processing parameters, that controls the heat input and heat distribution in the material. The main parameters, which impact on it are the temperature  $T$  and the effective time of action  $t_{eff}$ . In case of multipulsed nanosecond laser irradiation, temperature  $T$  on the surface can be calculated via estimation the solution of heat equation (Veiko et al. 2014, p. 343):

$$T(N_x) = \frac{2I_0(1-R)\sqrt{a}}{k\sqrt{\pi}} \sum_{n=0}^{N_x} \left[ \sqrt{t(N_x) - \frac{n}{f}} - \sqrt{t(N_x) - \left(\frac{n}{f} + \tau\right)} \right] + T_0 \quad (2)$$

where  $I_0$  is the density of radiation power,  $\tau$  is the pulse duration,  $f$  is the repetition rate,  $T_0$  is the initial sample temperature,  $R$  is the reflectivity on wavelength of  $1.06 \mu\text{m}$ ,  $k$  is the material thermal conductivity,  $a$  is the material thermal diffusivity.

Effective time of action is characterized by number of pulses per spot with diameter  $d_0$  according

to the formula (Veiko et al. 2014, p. 343):

$$t_{x,y} = N_x N_y \tau = \frac{d_0^2 \tau f N}{V_{sc}} \quad (3)$$

where  $N_x$ ,  $N_y$  are the number of pulses per spot with a diameter  $d_0$ ,  $V_{sc}$  is the scanning speed,  $H$  is the hatch distance.

Therefore, the number of pulses per spot equal to the focal spot diameter along axis X and Y can be calculated by the equations 4 and 5 respectively. The overlap along the X axis is programmed via the frequency  $f$ , along the Y axis through the resolution  $N$  expressed in the number of lines per  $mm$ . During the movement of the beam along the Y axis, there is no generation of radiation. Number of pulses per spot along axis X and Y can be calculated correspondingly:

$$N_x = \frac{d_0 f}{V_{sc}} \quad (4)$$

$$N_y = d_0 / H \quad (5)$$

Since  $N_x$  and  $N_y$  include all the necessary laser processing parameters, it is convenient to use them to define the different regimes together with the power density  $I_0$  which can be found from the well-known equation:

$$I_0 = \frac{4P}{\pi d_0^2} \quad (6)$$

Where  $P$  is laser power,  $d_0$  is spot diameter.

To estimate the power density of laser irradiation it is necessary to know the laser beam diameter. Laser beam cannot be focused in infinitely small area, there is a minimal diameter of the focused beam that can be achieved. In general, this diameter is related to diffraction limitations and parameters of used optics and depends on radiation wavelength and an aperture.

Fiber lasers have rather good beam quality and can be sharply focused into the surface. For the developed laser processing system with the 100  $mm$  lens parameters of laser beam were measured with the use of beam profiling system. The result of caustic calculations is presented in figure 9. As it was found, the minimal radius for the applied optics and introduced experimental setup is approximately 13  $\mu m$ .

However, to guarantee better heat distribution and avoid deep penetration of the beam into the material the laser was focused a bit under the surface. Therefore, more uniform surface with better quality of the colored product can be reached. Also, more regular color can be produced. Thus, the laser beam diameter found for this work is  $40\ \mu\text{m}$ .

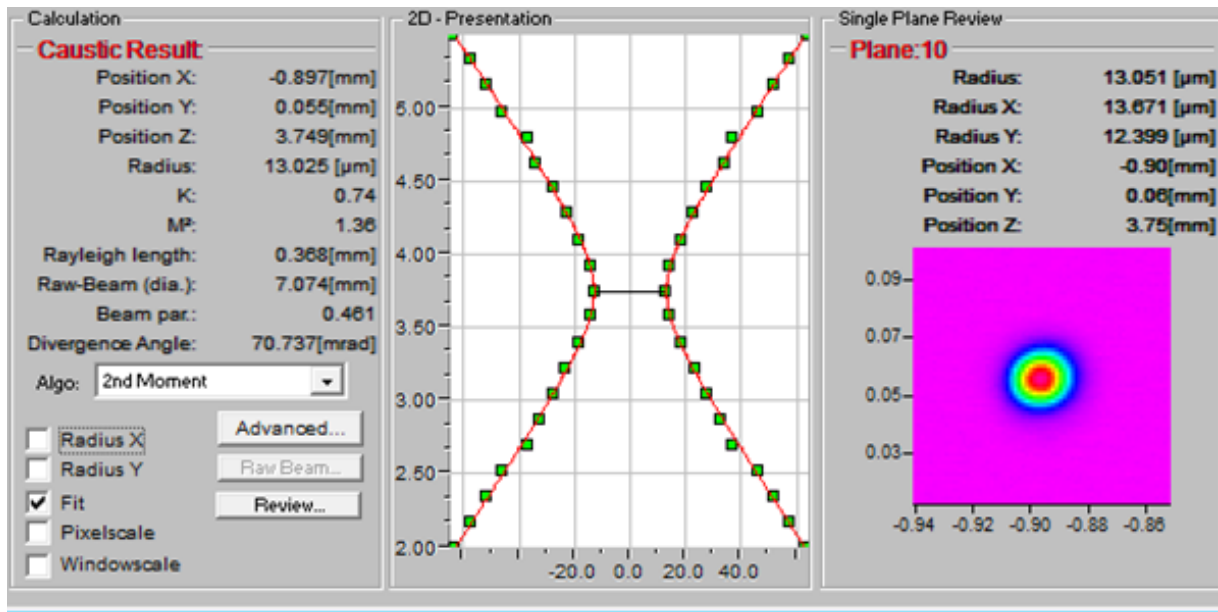


**Figure 9.** Caustic results

### 3.2 Spectrophotometry

All the colorimetry measurements and calculations were done in ITMO University, Department of optical-electronic devices and systems.

Reflectance spectra of the material before and after laser treatment were measured with Ocean Optics CHEM4-VIS-NIR USB4000 spectrophotometer (fig. 10). This device has good characteristics and resolution for visible spectrum wavelengths: signal-to-noise ratio - 300:1, integration time - 20ms, slit -  $5\ \mu\text{m} \times 1\ \mu\text{m}$ .



**Figure 10.** Spectrophotometer for measuring the reflectance spectra (Ocean Optics Inc. 2016).

To measure the spectral characteristics and color parameters of the obtained colors in the scanning mode the XY coordinate stage was implemented. The functional block diagram of the whole measuring setup is shown in figure 11.

A halogen lamp of 15 V with the filament dimensions of 360x2000 nm can provide the defined form of spectral distribution and is used as the source of illumination (1). Via optical fiber (2) light delivers into the entrance window of the illumination device integrated in the probe tool (3). The illumination device provides uniform illumination of the point on the surface of studied sample (4). After the reflection from the surface, light comes into the entrance window of the extraction device, which is implemented in the same probe chassis as the illumination device. From this extraction device the signal delivers via probe optical fiber (5) into the slit of the spectrophotometer (6). Both illumination and probe fibers have the diameter of 200  $\mu\text{m}$ . The spectrophotometer forms the packages of data by analyzing of input signal and transmit it to the microcontroller built-in the PC (7). This microcontroller defines the operating parameters of the spectrophotometer and calculates the result. For the analyzing and visualization of the measurements specialized software developed in LABView programming environment is utilized.



On the other hand, to achieve the precision movements of samples within the working field, the two-dimensional coordinate table (8) from STANDA is used. This stage provides the movements of flat sample in the field with size up to  $150 \times 150 \text{ mm}$ . Special microcontroller (9) provides the connection between the coordinate table and PC, thus, makes possible to synchronize the measuring tool and manipulations of the sample.

Implemented in the used spectrophotometric system linear CCD (Charge-coupled device) is based on several elements of the radiation detector. Taking into account the unstable temperature distribution of the environment, which can vary during the measurement, there is a need to calibrate the equipment before each series of measurements. The calibration consists of determining and recording the noise distribution parameters (removing zero signal) and updating the measurement of the reference spectral distribution (distribution of the light source - halogen lamp).

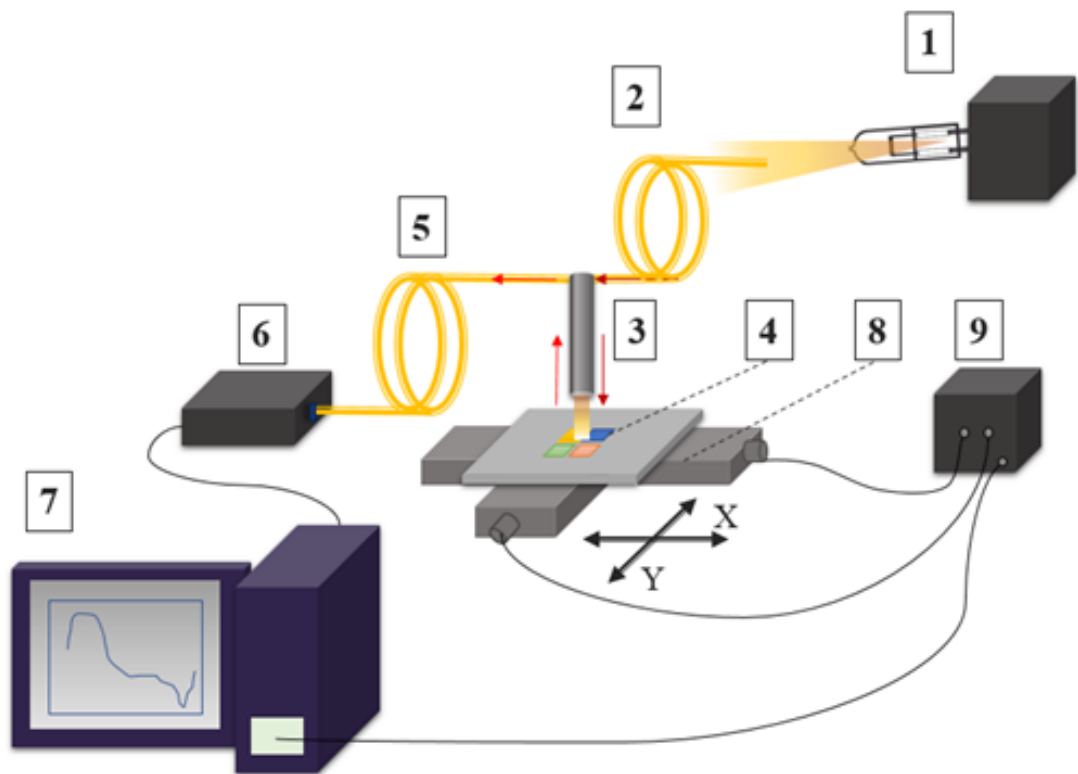


**Figure 11.** The functional diagram of the spectrophotometric measurement tool with the XY coordinate table. 1 – halogen light source; 2 – illumination optical fiber; 3 – probe; 4 – studied sample; 5 – the probe optical fiber; 6 – spectrophotometer Ocean Optics; 7 – PC; 8 – two-dimensional coordinate table Standa; 9 – driver and microcontroller for the coordinate table.

Due to the illumination device and the extension device are integrated inside the one probe tool, there is the possibility of simultaneous measuring of both specular and diffusion components of the signal. Thus, the measuring tool provides the possibility of analyzing the diffuse or specular spectral distribution of reflection coefficient and diffuse or specular spectral distribution of albedo. Also, it is possible to calculate the color coordinates of the sample in each probe point of the sample according to the different standards.

### 3.3 Color notation and calculations

As is well known, the reflection coefficient  $\rho$  characterizes the ability of the object's surface to reflect the radiation incident on it from the source. Quantitatively, the reflection coefficient can be expressed by the following relation (Sharma 2004, p. 185):

$$\rho = \frac{\Phi}{\Phi_0} \quad (7)$$

Where  $\Phi_0$  is radiant flux of initial irradiation,  $\Phi$  is radiant flux reflected from the object.

Due to the object can have different surface roughness, the reflection coefficients of specular  $\rho_r$  and diffuse  $\rho_d$  can also be determined.

The relative spectral distribution of the reflection coefficient  $\beta(\lambda)$  is used to determine the color of any object, and can be calculated from the ratio:

$$\beta(\lambda) = \frac{\Phi_{ob}(\lambda)}{\Phi_s(\lambda)} \quad (8)$$

Where  $\Phi_{ob}(\lambda)$  is the relative spectral distribution of the light source radiant flux reflected from the surface of the object;  $\Phi_s(\lambda)$  is the spectral distribution of the radiant flux of the light source reflected from the reference white surface.

Thus, the color coordinates X, Y, Z are the defined colorimetric parameters of the object, that are determined by the following parameters: the relative spectral distribution of the reflection coefficient  $\beta(\lambda)$ , the spectral distribution of the radiant flux of the light source S ( $\lambda$ ) and the color matching functions of the CIE XYZ system ( $x(\lambda)$ ,  $y(\lambda)$  and  $z(\lambda)$ ). (Gorbunova et al. 2015.)

The color coordinates X, Y, Z can be defined by the following formulas:

$$X = k \int_{\lambda=360}^{\lambda=830} S(\lambda)\beta(\lambda)\bar{x}(\lambda)d\lambda \quad (9)$$

$$Y = k \int_{\lambda=360}^{\lambda=830} S(\lambda)\beta(\lambda)\bar{y}(\lambda)d\lambda \quad (10)$$

$$Z = k \int_{\lambda=360}^{\lambda=830} S(\lambda)\beta(\lambda)\bar{z}(\lambda)d\lambda \quad (11)$$

Where k is the normalizing factor, calculated by the equation12:

$$k = 100 / \int_{\lambda=360}^{\lambda=830} S(\lambda)\bar{y}(\lambda)d\lambda \quad (12)$$

The calculated color coordinates X, Y, Z can be converted to the relative color coordinates x and y or to any other color coordinate system, for example, to the CIE RGB system where a source of type D65 is a standard of natural light.

#### 3.4 Other methods

The explained method of laser metal coloration is related to not only applying the covering to the surface, but physical and chemical modification of the material. Since that, it is necessary to study the surface topology before and after laser treatment. There are many different methods to analyze the surface.

In this work, the visual analysis of the samples in microscale the optical microscope Carl Zeiss Axio Imager A1M is applied. The microscope is equipped by lenses with the different magnification in the range of 20x to 100x power. Due to good resolution, it is possible to examine the oxide film morphology and the properties of oxides.

For the more detail examination of the treated surface the SEM (scanning electron microscope) JEOL JSM 7001F was used. The microscope has good lateral resolution of approximately 1  $\mu\text{m}$ . The information depth depends on the accelerating voltage and the material characteristics and for this particular case it varied in the range of 0.2–1  $\mu\text{m}$ .

To determine 3D topology of the obtained area and the topology profiles were characterized by atomic force microscopy (AFM) Veeco Dimension 3100 in contact mode. Using a NanoScope IIIa controller and Quadrex signal processor the resolution of 16-bit on all 3 axes can be achieved.

To determine how different possible weather conditions such as extremely high and low temperatures and high and low humidity affect on the quality of the colors, special tests with the exposure the samples in the environmental chamber were done. SM-3200 Benchtop Environmental Chamber from Thermotron was used for this purpose. The chamber is equipped with an electronic humidity sensor which allows to control the value of humidity with the high accuracy. This chamber has the temperature range of -40 to 130 °C and the humidity range of 20% to 95% RH. The possible temperature-humidity overlap is shown in figure 12.

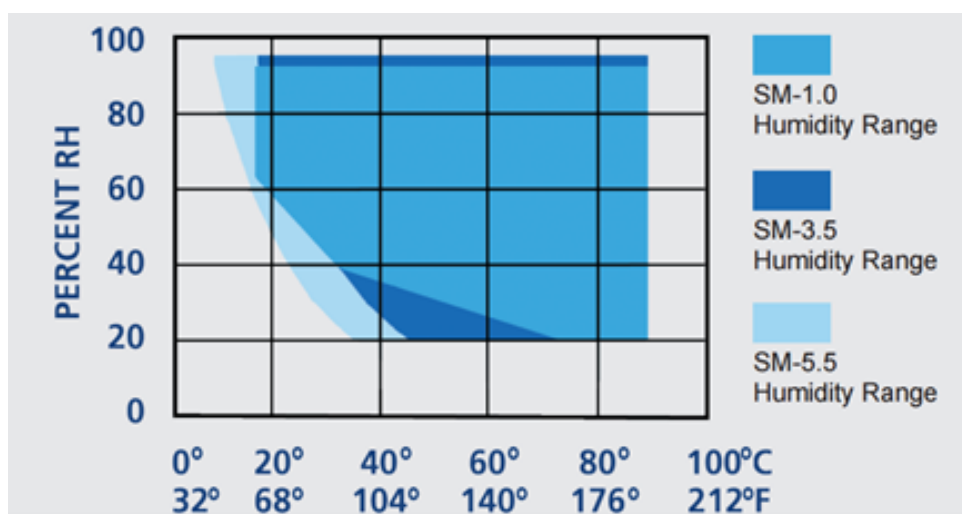


**Figure 12.** Temperature-humidity range for the environmental chamber SM-1.0 3200 Benchtop

Samples were also examined with the microhardness tester PMT-3M from LOMO (Leningrad Optical Mechanical Association). The value of hardness can be determined with a very high accuracy due to wide load range from 0.0196 to 4,9 *N*. The tester equipped with microscope with the possible magnification to 130, 500 and 800x what allows to measure even very small indents.

Thus, full analysis of the surface before and after treatment is presented in this work.

## 4 OBTAINING OF COLOR PALETTE

This chapter involves the description of the color marking process, dependencies of produced colors on different processing parameters, optical and physical properties of the obtained marks.

### 4.1 Development of color palette

For color laser marking the values of intensities under the melting threshold of the material are used. Thus, the process includes consequent melting and re-solidification of the material, that leads to various chemical reactions on the surface, including oxidation and nitridation.

Under the influence of laser radiation, a melting pool is formed on the surface of the material (fig. 12 a). In this case, the molten material from the center of the melt area usually moves under the action of the recoil pressure of the vapors to the periphery, where, due to the surface tension forces, a roller grows. The formation of the oxide films occurs on the surface of this roller as well as on the walls of the produced cavity. The modified area has a form of a microdisk (fig. 12 d). The next pulse heats the area again, and depending on the proportion of the overlap the final heat distribution could be different (fig. 12 c). In general, the material does not have enough time to cool between two pulses due to conductivity and temperature rises from pulse to pulse gradually. Therefore, the microstructure that was formed by the previous pulse would be erased and re-formed again by the next pulses (fig. 12 e). Thus, the final surface structure and the oxide film structure is a result of multiple pulsed laser action and will be different depending on laser heat imputes well as on the overlap value (fig. 12 e).

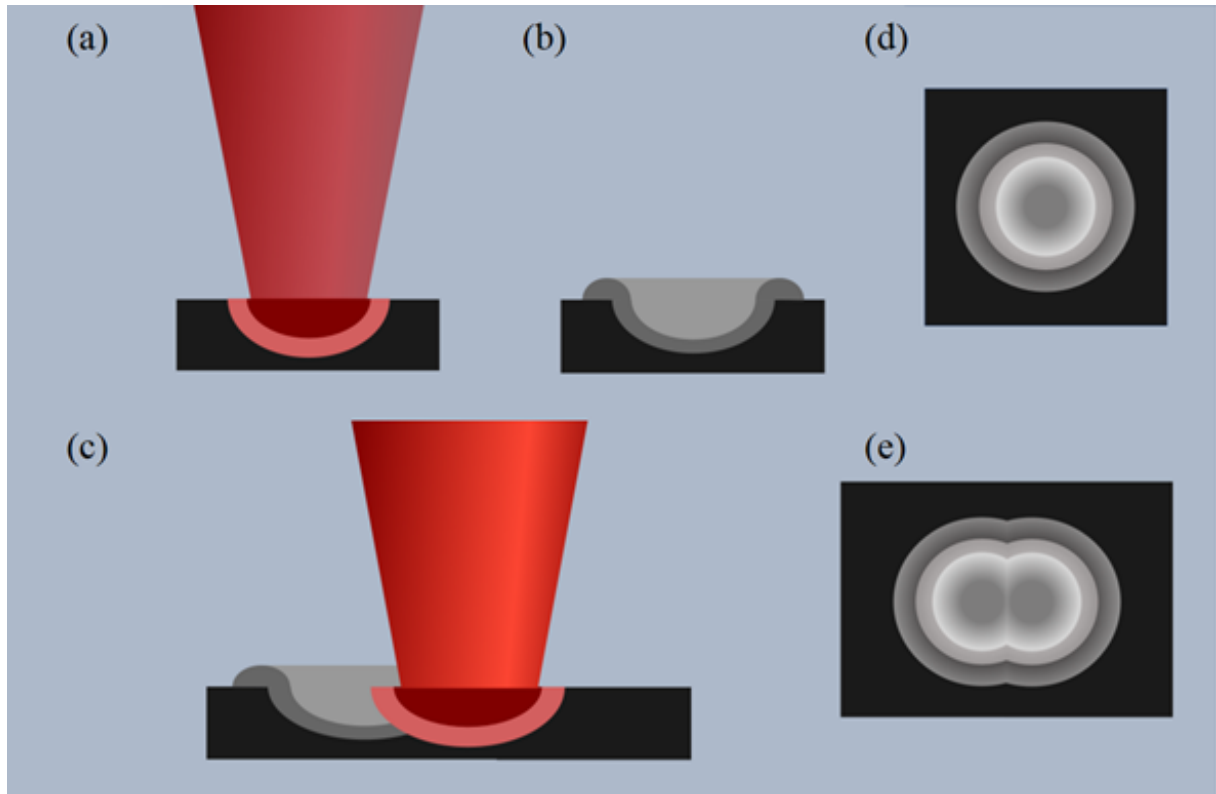


**Figure 13.** Mechanism of laser-material interaction: the pulse action - a, material surface after the first pulse - b, surface modifications during next pulses - c. View from above: after a first pulse - d, after next pulses - e.

The dependence of the resulting color on the surface relief is not the aim of current work and is considered in details in (Ageev et al. 2017b). Almost all the parameters of laser source and scanning might influence on the result: both on the relief and the color of the surface. In this work dependence of produced colors on the laser power, scanning speed, frequency of laser pulses and a pulse duration is investigated.

Firstly, the dependence of colors on the laser power (power density) vs scanning speed was studied. The result of laser marking with the following parameters is presented in fig. 14: pulse duration  $\tau = 100 \text{ ns}$ , frequency  $f = 60 \text{ kHz}$ , hatch distance  $H = 0.01 \text{ mm}$ , laser power density in the range of  $8 \cdot 10^7 - 1.6 \cdot 10^8 \text{ W/cm}^2$  with the step of  $0.8 \cdot 10^7 \text{ W/cm}^2$  from the top to the bottom; scanning speed from  $300$  to  $750 \text{ mm/s}$  with the step of  $50 \text{ mm/s}$ .



**Figure 14.** The dependence of produced color on the power densities  $I_0 = 8 \cdot 10^7 \div 1.6 \cdot 10^8$   $W/cm^2$  from up to bottom; scanning speed  $450 \div 900$   $mm/s$ ,  $f = 60$  kHz,  $\tau = 100$  ns,  $H = 0.01$  mm.

As it was found, colors are not changes significantly with the increasing the power, only parametric window for each color moved to the higher scanning speed values. Since the better productivity can be achieved at higher intensities because this way the scanning speed can be increased significantly, more detailed experiment had been required for these regimes. Therefore, the next step was the dependence of color on the scanning speed with the fixed maximal available value of power which is 20W. Other parameters (frequency, pulse duration, hatch distance) were the same. Scanning speed was changed in the range of 450-850  $mm/s$  with the step of 10  $mm/s$  (the first four lines in fig. 15) and then with the same step from 50 to 150  $mm/s$  (fifth line in fig. 15).



**Figure 15.** The dependence of produced color on the scanning speed.  $I_0 = 1.6 \cdot 10^8 \text{ W/cm}^2$ ;  $f=60\text{kHz}$ ;  $\tau=100\text{ns}$ ;  $H=0.01 \text{ mm}$ ; scanning speed  $450 \div 850 \text{ mm/s}$  (line 1 to 4),  $50 \div 150 \text{ mm/s}$  (line 5) from left to right.

Indeed, it can be found, that with the increasing of the scanning speed colors change in the following order: from dark green, then dark violet, wine red, orange, light green, gold and light blue. For low scanning speeds only dark gray colors occur.

As it was noticed in general colors change gradually from one to another passing different shades. However, some of presented regimes are not so stable. For example, when color changes from orange to light green ( $3^{\text{rd}}$  line,  $7^{\text{th}}$  square) the conversion is not uniform. It is necessary to avoid this kind of parametric windows for the final palette as it can cause faults in marks.

To expand the color palette, the test with the various frequencies was also performed. In the fig. 16 the dependence of color on scanning speed for the different frequencies is shown. The parameters were chosen as following: intensity  $I_0 = 1.6 \cdot 10^8 \text{ W/cm}^2$ , pulse duration  $\tau = 100\text{ns}$ , hatch distance  $H=0.01 \text{ mm}$ , scanning speed  $450\text{-}1200 \text{ mm/s}$  with a step of  $50 \text{ mm/s}$ . The values of frequencies were change from up to down each to lines 100, 200, 500 and 1000  $\text{kHz}$  correspondently.



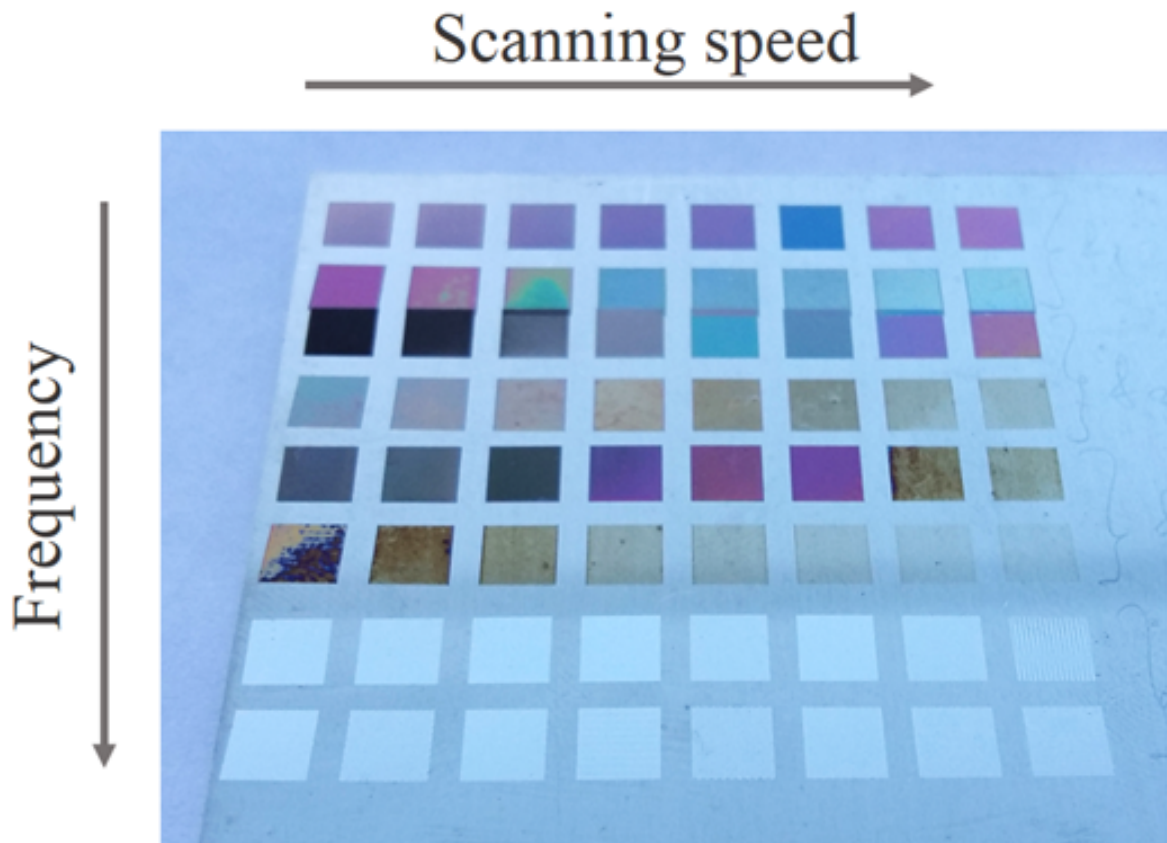


**Figure 16.** The dependence of produced color on the scanning speed for the different frequencies.  $I_0 = 1.6 \cdot 10^8$ ;  $\tau = 100 \text{ ns}$ ;  $H = 0.01 \text{ mm}$ ; scanning speed  $450 \div 1200 \text{ mm/s}$ ,  $f = 100 \text{ kHz}$  (lines № 1,2);  $f = 200 \text{ kHz}$  (lines № 3,4);  $f = 500 \text{ kHz}$  (lines № 5,6);  $f = 1000 \text{ kHz}$  (lines № 7,8).

The experiment with different frequencies showed that some unique colors such as aquamarine (1<sup>st</sup> line, 6<sup>th</sup> square), light pink (2<sup>nd</sup> line, 1<sup>st</sup> square) or bright purple (5<sup>th</sup> line, 6<sup>th</sup> square) might be obtained with higher frequency regimes. In general, produced colors are not so uniform as for the lower frequency and there is no subsequent conversion of colors is observed.

For the  $f = 1000 \text{ kHz}$  only silver colors occur for the all scanning speed range. It might be caused by too high scanning speed. Thus, the parametric window for producing different colors at this frequency was not found during the experiment. However, white or silver color is rather fast in this frequency range, that can be utilized for the final palette.

One more parameter to change was the pulse duration. It is well known that the shorter the pulse duration, the smaller the heat affected zone in the material. Thus, the temperature distribution will be different for shorter pulses and it results in the producing colors. The result of tests with

the different pulse durations for the vary scanning speed is shown in fig. 17. Laser processing parameters were as following: intensity  $I_0 = 0.8 \cdot 10^7, 1.6 \cdot 10^7 \text{ W/cm}^2$ , pulse duration  $\tau = 4, 8 \text{ ns}$ , hatch distance  $H=0.01 \text{ mm}$ , scanning speed  $50\text{-}200 \text{ mm/s}$  with a step of  $10 \text{ mm/s}$ .

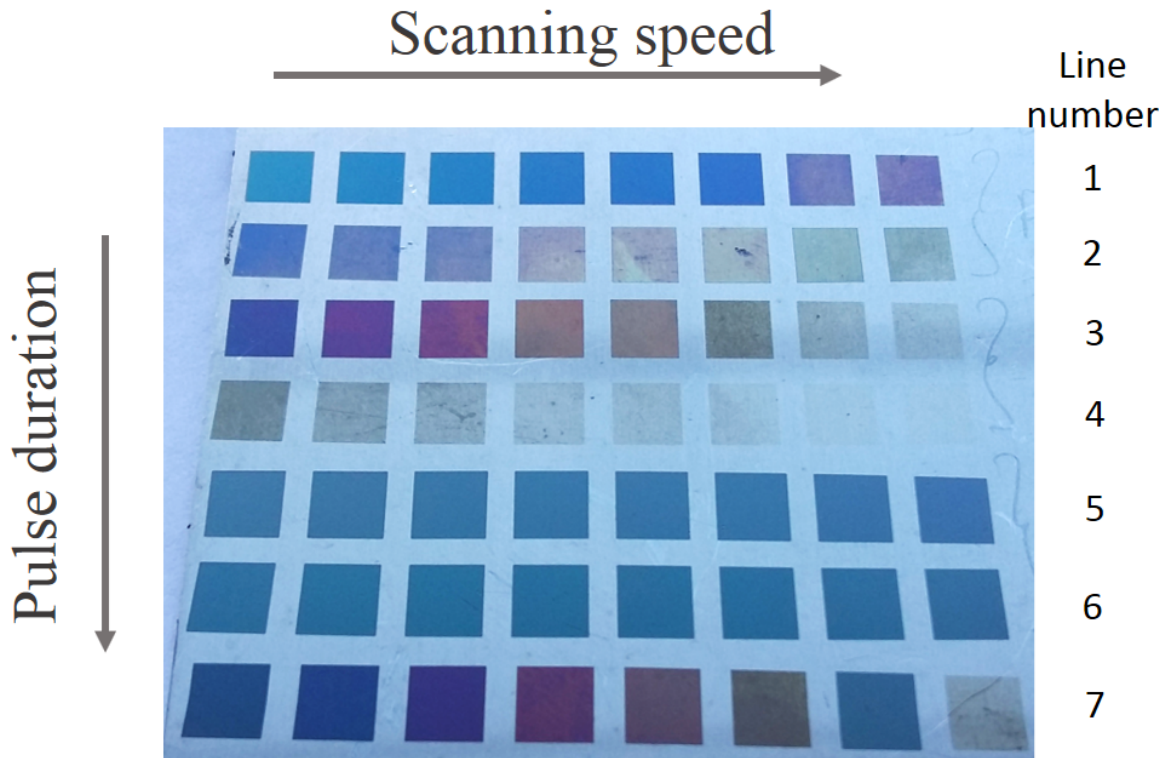


**Figure 17.** The dependence of produced color on the scanning speed for the different pulse durations:  $H=0.01 \text{ mm}$ ; scanning speed  $50\div 200 \text{ mm/s}$ ,  $f=60 \text{ kHz}$ ;  $\tau=4 \text{ ns}$ ,  $I_0 = 0.8 \cdot 10^8 \text{ W/cm}^2$  (lines № 1,2);  $\tau=4 \text{ ns}$ ,  $I_0 = 1.6 \cdot 10^8 \text{ W/cm}^2$  (lines № 3,4);  $\tau=8 \text{ ns}$ ,  $I_0 = 0.8 \cdot 10^7 \text{ W/cm}^2$  (lines № 5,6);  $\tau=8 \text{ ns}$ ,  $I_0 = 1.6 \cdot 10^8 \text{ W/cm}^2$  (line № 7).

The pulse duration has strong impact on the color. The sequence of the colors appear is different for shorter pulse durations and shades are different. Basically, colors come in such order: light blue, aquamarine, bright blue, green, purple, orange and yellow. This order corresponds to interference colors that are result of differences in oxide film thicknesses which are grown due to defined laser heat input and time of action. In this case, the color can correspond to different orders of interference. Precise control of the parameters of laser radiation makes it possible to produce colors that can not be obtained by thermal methods. Sometimes bright pink and dark blue can be obtained.

The second big difference is the roughness of the surface under the colors. For long pulses

( $\tau \gg 20 \text{ ns}$ ) visually colors are glassy and the material under them is smoother than for shorter pulses. On the other hand, with the shorter pulses the parametric window moves to the lower scanning speed values, that decreases the productivity of marking.

For the pulse duration values of  $4 \text{ ns}$  and  $8 \text{ ns}$  almost the same color dependence is observed. However, for  $8 \text{ ns}$  scanning speed is more than for  $4 \text{ ns}$  and generally, colors are more uniform. Some regimes have a wide parametric window that is positive for the production, since it can decrease the possibility of a mistake.

Therefore, for each dependence the results were analyzed and parametric windows for the most interesting colors were found. Based on this observation, the color palette of fifteen different shades was formed. Parameters for colors were chosen in the middle of the parametric window to provide more stability to the process. Moreover, each color was checked for the repeatability, i.e. it was made in the different sites of the working field. Also, the different size squares were marked to avoid the size effect which is the spontaneous modification of the color depending on the size and shape of the picture to be marked. Thereby, parameters of some colors were adjusted to provide more stability for the marking process. Therefore, parameters of the colors which were selected for the final color palette are shown in table 3. Here the number of pulses per spot ( $N_x, N_y$ ) and power density are used as this values include all the necessary processing parameters.

*Table 3. Processing parameters for the final color palette.*

<b>Number</b>	<b><math>N_x</math></b>	<b><math>N_y</math></b>	<b><math>I_0, 10^8 \text{ W/cm}^2</math></b>
1	13	4	0.8
2	7	4	1,6
3	44	4	1,6
4	11	4	1,6
5	10	4	1,6
6	44	4	1,6
7	57	4	1,6
8	8	4	1,6
9	7	4	1,6
10	4	4	1,6
11	4	4	1,2
12	3	4	1,2
13	22	4	1,6
14	200	4	1,6
15	24	4	1,6

Thus, fifteen basic colors for stainless steel AISI 304 were produced by color laser marking technology. The visual appearance of the color palette is performed in figure 17. Colors have a uniform structure and include almost all the basic colors of spectrum. Obtained colors have an interference nature, depending on the light incident angle as well as the position of an observer colors could have the different visual appearance. Thus, in figure18 photo has been taken from the different angles. This effect can be increased due to irregular surface structure of processed steel (Ageev et al. 2017a).

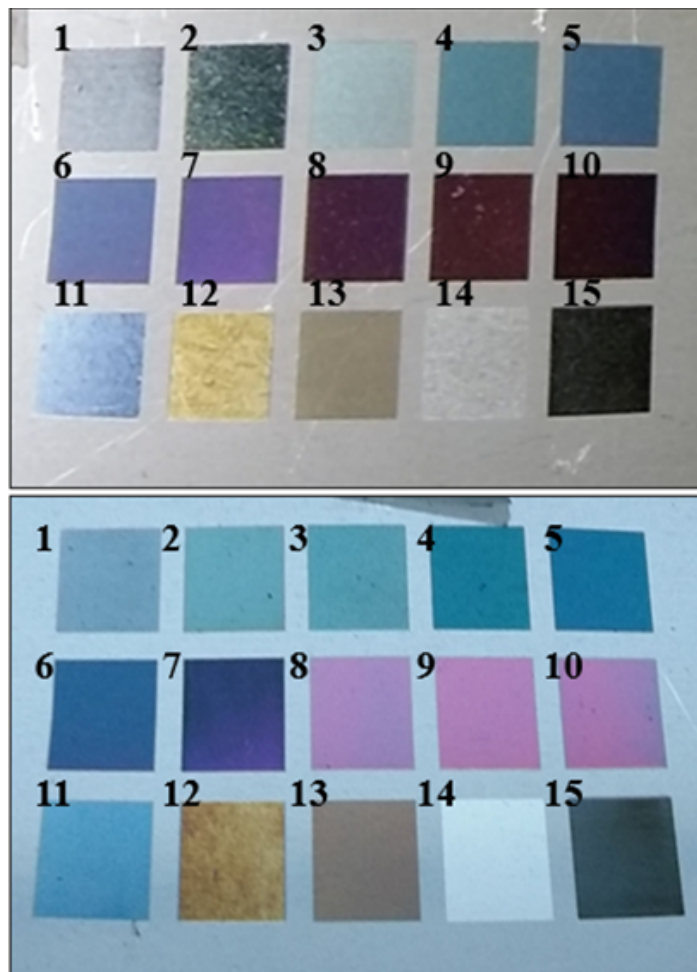


**Figure 18.** Final color palette for stainless steel AISI 304.

It is obvious that depending on the position of the focal point colors will change due to focal point position variation of the system. To determine the maximum value of this variation which is not affect on colors, the color palette was reproduced with a different displacement of the focus point from the working position in millimeters. The result is shown in figure 19, where values in white blocs are displacement. According to these results, the maximum displacement which is acceptable for the technology is  $\pm 0.2 \text{ mm}$ .

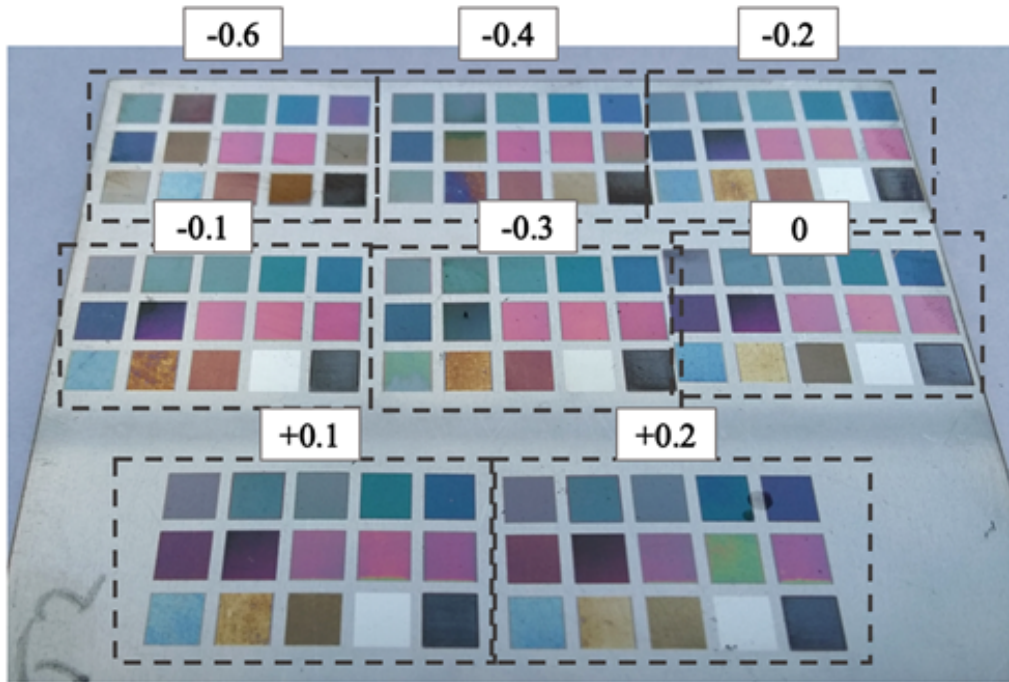


**Figure 19.** Dependence of color on the displacement of the focus point. Values in white blocks represents the displacement value from the original position (zero) in millimeters. Plus sign means the displacement to the surface, minus is the displacement from the surface.

Each square has the dimensions of  $8 \times 8 \text{ mm}$ . The time to produce one color palette of fifteen colors is approximately 5 minutes. The productivity of the process is rather high in corporation with another metal color marking techniques if the time of preparation is taken into account. However, it can be increased for about 30% by adjusting the processing parameters and for more than 100% with applying more powerful laser source. For this work it was not the main goal and received productivity was high enough for the desired results.

#### 4.2 Analysis of obtained structures

To observe the microstructure of obtained colors as well as to analyze the oxide film structure for the color palette an optical microscopy was used. In figure 20 microimages of each color and the bear surface are shown.

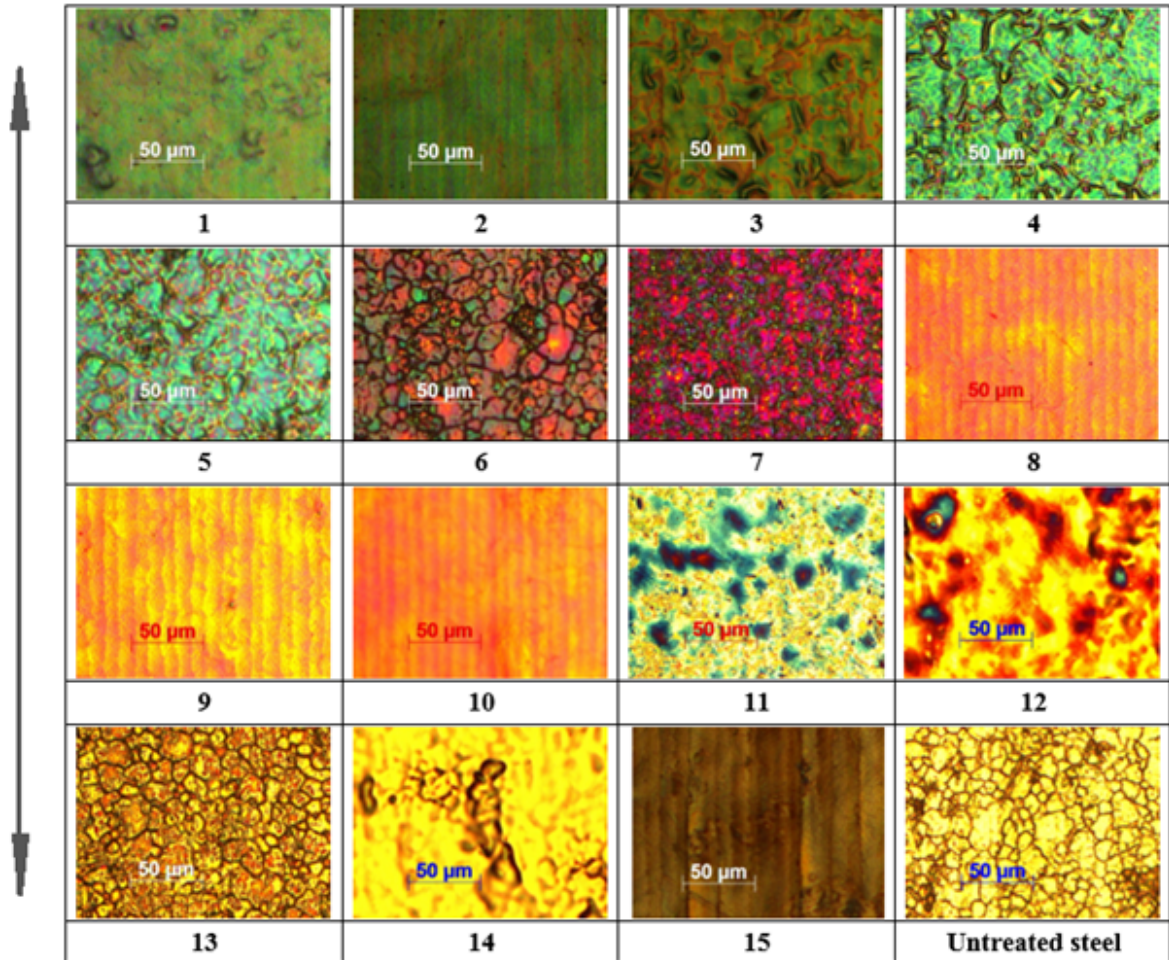


**Figure 20.** Microimages of the color palette on stainless steel AISI 304. Arrow shows the scanning direction.

By analyzing the microimages, it can be concluded that the samples obtained with large overlaps (high value of  $N_x$  and  $N_y$ ) consist of separate regions of different colors. The percentage of the inclusion of the same color defines the integral color of the surface that we can observe visually with the naked eye. The more inclusions of one color at the microscale there is and the larger they are, more homogeneous the resulting color is.

It can be concluded from the analysis of microimages, that depending on the regime of laser processing and overlapping, the structure of the oxide film will be different. Some samples, for instance 8-10, 15, have strongly marked periodic microstructures, which are related to scanning passes. Others (11, 12, 14) have irregular microstructures, that can probably be related to multiple melting and re-solidification of the surface. The third type is a grained-like structure, which is representative for samples 6 and 7. These structures are similar to the untreated stainless

steel sample and can be result of minimal melting of the material, thus, the oxidation in this case occurs under the melting threshold.

To investigate structures more detailed, SEM of some images were taken. All the images were done with the accelerating voltage of the electron beam of 5kV. The result for the different samples is shown in figure 21.

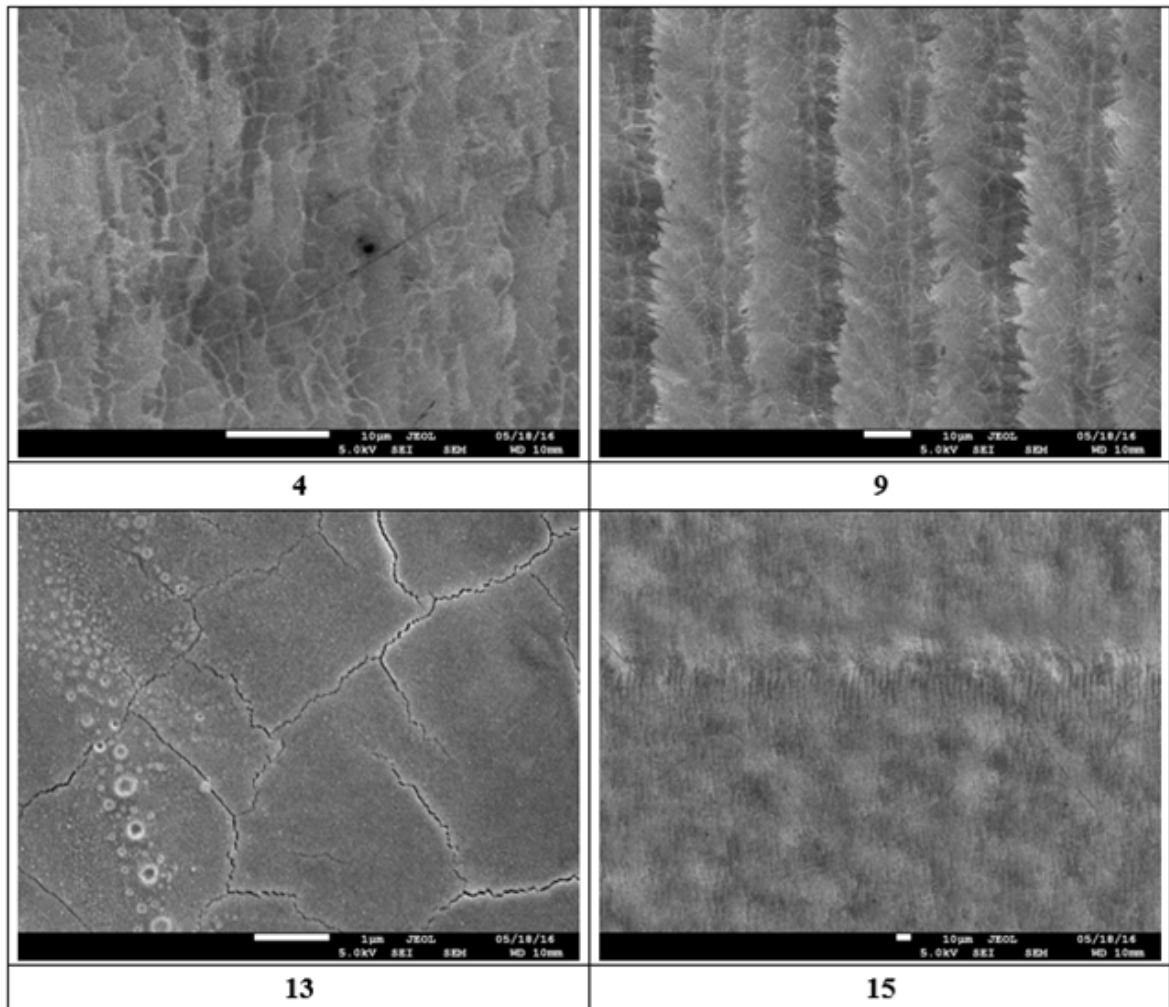


**Figure 21.** SEM images of the samples.

As it was suggested previously, for different laser processing parameters the different types of microstructures can be observed. However, both optical microscopy and SEM techniques cannot give the information about the surface topology. Hence, produced structures were also studied by AFM in contact mode. For the examination, the sample number 9 was chosen since visually it has the most developed relief. Surface profile figure (a) and 3D plane of the sample (b) are shown in figure 22.

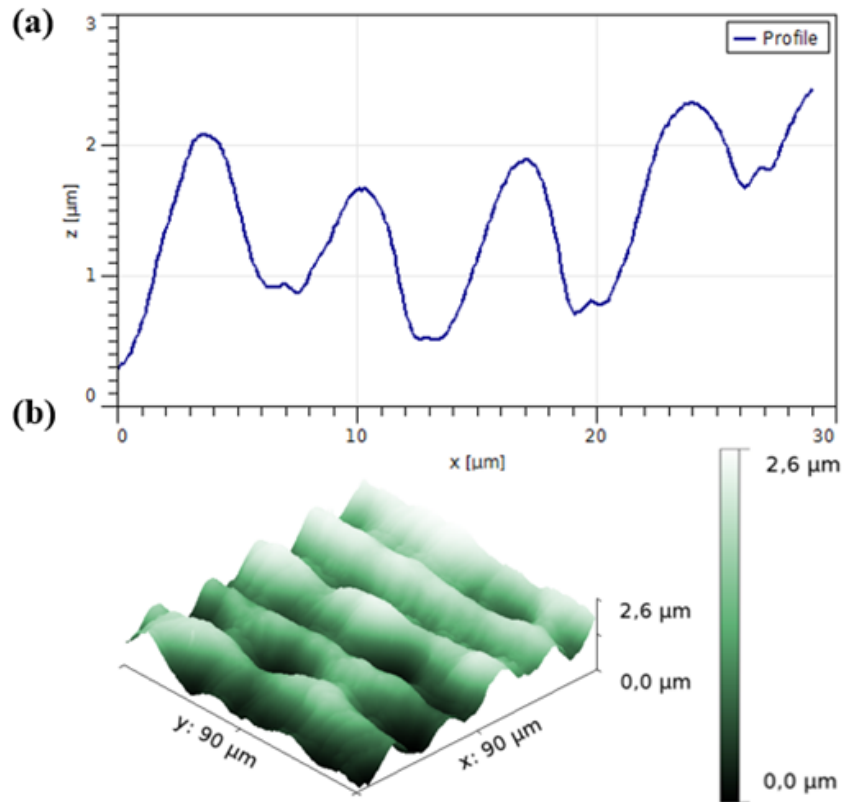


**Figure 22.** AFM study of the sample 9: profile - a; 3D plane - b.

Indeed, as it was described previously, the sample has periodically iterative relief that is related to the scanning geometry. The high of these structures reach the value of approximately  $1.5 \mu\text{m}$  what is relatively small in comparison with the own surface roughness of the material. Hence, it should have a negligible effect on the material.

The chemical composition of obtained samples can be determined by the different methods, including analytical thermodynamics method (Ageev et al. 2017a), EDX (Energy-dispersive X-ray spectroscopy) analysis (Adams et al. 2013), XRD analysis (Cui et al. 2008) and Raman scattering spectra (Amara, Haïd & Noukaz 2015). For the current work, the last method was used.

The experiment was carried out by means of Center of Optical and Laser Materials research of Saint Petersburg State University Research park. Raman scattering analysis involves the laser exposure of an experimental sample and analyzing of the scattered irradiation. Using special filters it is possible to extract weak Raman scattering from strong Rayleigh scattering.

For the experiment the solid-state laser with the wavelength of  $532 \text{ nm}$  and output power of



approximately 1 mW was utilized to initiate scattering from the surface of sample to be study. The radiation of the probe laser is too low to destroy or make any effect on the samples.

Samples 9 and 13 were examined for the determination of the chemical composition. For a detailed analysis, consider example number 9 which spectrum is shown in figure 23. To accurately determine the position of peaks the Lorentz fitting function was applied to the graph. Therefore, 7 Lorentzian peaks were determined at 288, 332, 390, 541, 634, 674 and 715  $cm^{-1}$ .

According to the (Gardiner et al. 1987, p. 62)  $FeCr_2O_4$  has the own phonon modes, which locates with a very good much with the 541, 634, 674  $cm^{-1}$ . That means the presence of  $FeCr_2O_4$  in the obtained films. Other peaks at 288, 332, 390 and 715  $cm^{-1}$  correspond to the presence of maghemite ( $Fe_2O_3$ ) or maghemite-rich region (Thibeau, Brown & Heidersbach 1978, p. 533), that can be related to both the oxide film as well as the untreated steel. In general, the results confirm the previous studies in this field.

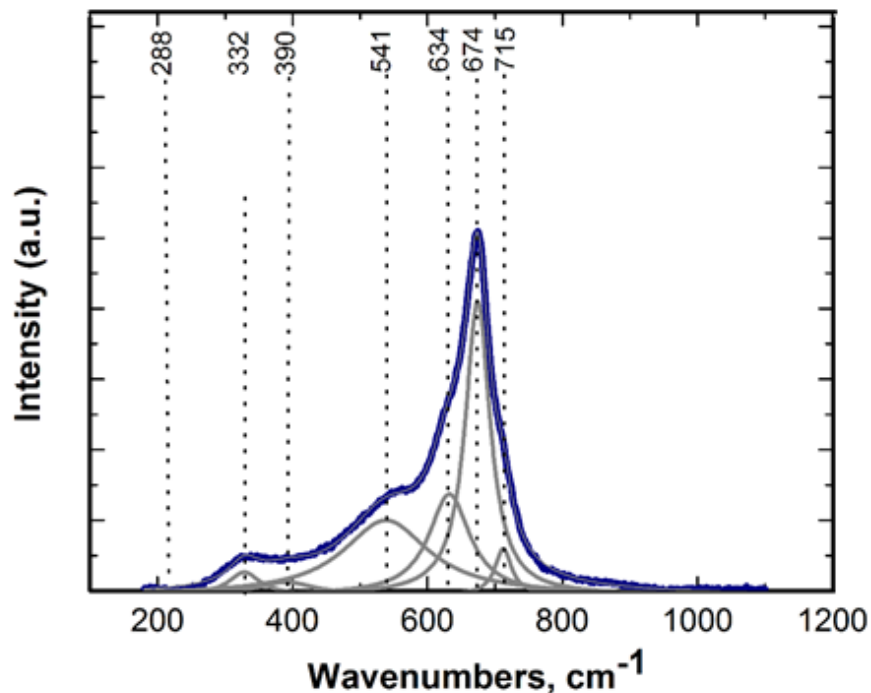


**Figure 23.** The Raman spectra of the sample №9. Gray lines mean the Lorentz profiles to fit the function.

In conclusion, twenty same samples of stainless steel AISI 304 were produced according to the described technology. Each sample has fifteen squares of different colors with the dimensions

of 8x8 mm.

The grown oxide films were investigated using optical microscopy, SEM, and surface topology was described by AFM. Analysis showed that depending on laser processing parameters four main types of oxide structures were produced. According to the Raman spectrometry, oxide film consist of  $FeCr_2O_4$  and  $Fe_2O_3$ .

## **5 TESTING FOR REPETABILITY AND WEAR RESISTANCE OF COLORED SURFACE**

For implementation of any new technology to industry it should have a good price-quality ratio. Quality for the production plays very important role and has to be approved and be compliant with standards. For each industrial field and in different countries these standards can be dissimilar.

In the modern industry applying of the various coatings, the issue of quality control of the technological process is paramount. Negligent attitude on the procedures of operational and post-production control may result in spoilage of expensive equipment or structures during operation, which will entail huge losses of funds and time. Quality control of coatings is carried out in accordance with the standards for recommended methods with the use of specialized instruments.

To control the profile of the surface before and applying a coating, one can use a roughness standard or a roughness meter. Immediately after coating, its thickness can be examined by a measuring hexagonal comb or a disk for measuring the thickness of thin films. The thickness of the dry layer of protective or paint coatings can be measured using a digital thickness gauge of coatings and thickness gages of coatings of a destructive type. The degree of adhesion of the coating to the surface can be determined with the help of an adhesion measuring tool. To control the appearance of coatings online, a specialist can use a portable USB microscope. Also, different chemical methods are commonly applied to control the quality of the coatings.

All methods can be divided into destructive and non-destructive testing, depending on the amount of damage to the material. In this chapter, the results of different testing techniques, i.e. colorimetric measurements, hardness and scratching tests, environmental tests and some chemical resistance tests.

### **5.1 Repeatability of obtained colors**

In the first place, for color coatings significant importance have the repeatability of them from one production circle to another. Producers as well as consumers makes strict requirements to the quality of the color, its uniformity and in particular to the reproducibility of the same color. From this point of view, it is necessary to develop the method of monitoring which allows to control all the above properties.

First possible technique for determination the quality of color is the simple visual analysis. However, the color sensations of the eye are not stable. They depend on many factors, both physiological (the state of the retina, the size of the pupil), and psychological (the colors of the surrounding objects, the state of the observer). Obviously, there is no one-to-one relationship between physical radiation and color sensation, which means that we can not use visual observation as the standard method of the color analyzing. Therefore, the basis of color determination is the analysis of reflection and transmission spectra of objects.

Accepted color spaces are three-dimensional. It means that they depend on three coordinates, since the definition of a color with three parameters, for example, with color tone, saturation and brightness. (Chu, Devigus & Mielezsk 2004.)

The International Commission on Illumination (CIE) adopted a standard color coordinate system CIE XYZ based on determining the proportion of red, green and blue components in the past or reflected light. When mixing these three components at a wavelength region  $\lambda = 360-780$  nm, a white (monochromatic) radiation point is obtained.

In modern production nowadays it is often uses the recommended by CIE system CIE RGB. In it, as in the XYZ system, the red (R), green (G) and blue (B) flux components are used as coordinates. The RGB system is convenient for capturing colors by the camera and reproducing them on a monitor or projector.

The RGB color space can be represented in the form of a single cube, shown in Figure 24 . The points corresponding to the base colors are located at the vertices of the cube lying on the axes: red - (1; 0; 0); green - (0; 1; 0); blue - (0; 0; 1). In this case, secondary colors (obtained by mixing the two basic colors) are located at other vertices of the cube: blue - (0; 1; 1); purple - (1; 0; 1) and yellow - (1, 1; 0). Black and white colors are located at the origin (0; 0; 0) and the point (1, 1, 1) furthest from the origin. (Sharma 2004, p. 301.)

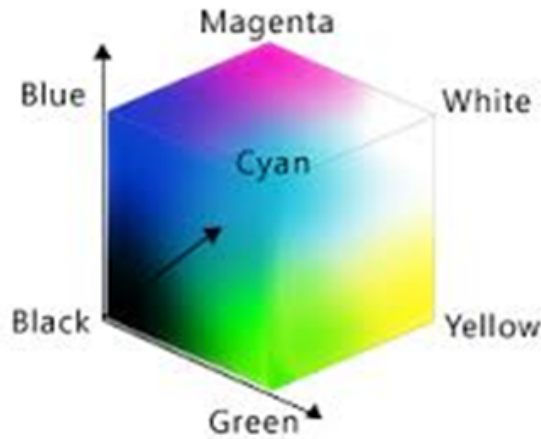


**Figure 24.** Color relationships in CIE RGB color space (Bostroem, Trevor & Stanevaa 2016).

Measured reflectance spectra of the samples is shown in figure 24. To define the colors in this system, the additive addition rule is used (Koenderink 2010, p.370):

$$C = r' \bar{R} + g' \bar{G} + b' \bar{B} \quad (13)$$

Where  $\bar{R}$ ,  $\bar{G}$ ,  $\bar{B}$  are the units of the corresponding primary colors  $r'$ ,  $g'$ ,  $b'$  are the color coordinates that show how many fractions (units) of each of the primary colors must be taken to form the given color C. Also, relative color coordinates calculated in the same way as in the CIE XYZ system (Koenderink 2010, p.371):

$$r = r' / (r' + g' + b') \quad (14)$$

$$g = g' / (r' + g' + b') \quad (15)$$

$$b = b' / (r' + g' + b') \quad (16)$$

Therefore, to control colors of obtained samples the standard CIE RGB coordinate space will be used. To calculate color coordinates the reflectance spectra of each color are supposed to be taken.

Reflection spectra of all samples representing a square of a color of 8x8 mm in size were taken using the setup described previously (fig. 11). Each colored square was divided into 25 regions as it shown in figure 25 . Firstly, the reflectance spectra of each region were taken. Then, the

final spectrum was determined by averaging the spectra of the selected regions (fig. 26).

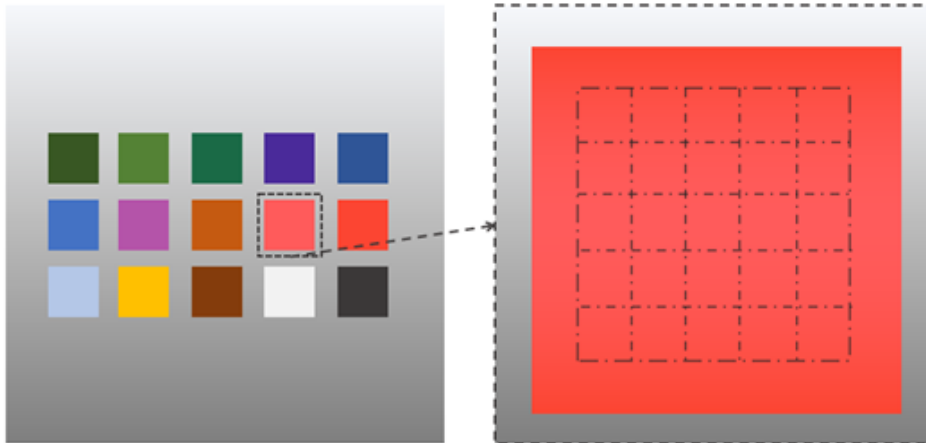


**Figure 25.** Scheme of color measurements.

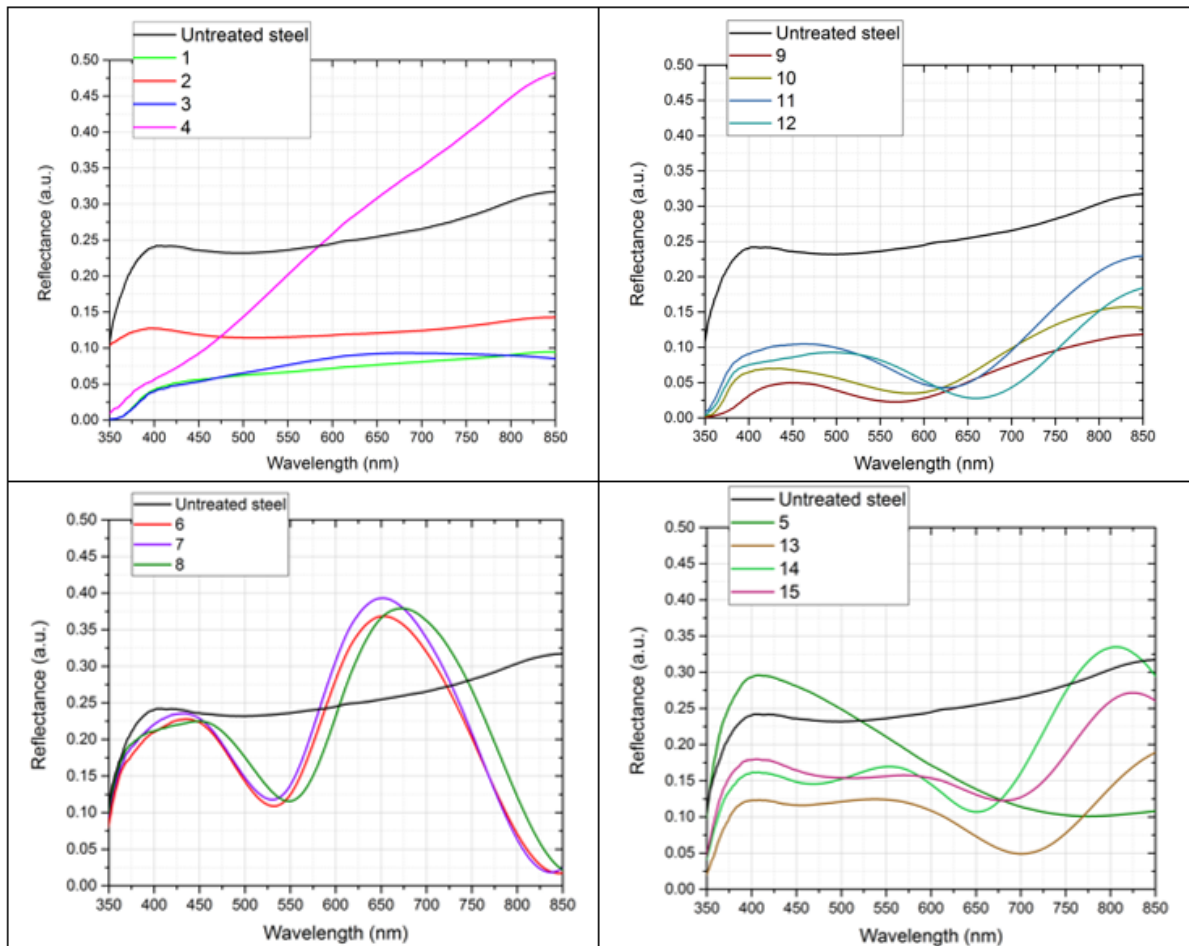


**Figure 26.** Reflectance spectra of obtained colors.

All the spectra can be divided into four groups. Firstly, it is a plane spectra (fig. 26a) These spectra do not have any evident peaks in visible wavelength range and the principal appearance

are similar to untreated steel spectra. Most likely colors of these group are related both to own oxide color and the color of surface due to small thickness of film. Then second group gets one clear peak between 500-700 nm (fig. 26b). Next group has two maximums around at 420 and 550 nm correspondingly (fig. 26c). Peaks of the last group are stretched in comparison with the previous group (fig. 26d). Appearance of peaks probably is related to interference effect in thicker oxide film and results in coloration of the surface. The color coordinates in CIE RGB color space for each square were calculated using the program developed in LABView programming platform. The result of calculations with a representation of each color is presented in table 4.

*Table 4. CIE RGB color coordinates of the colors from the final palette.*

Number of sample	Color coordinates		
	R	G	B
1	84	92	89
2	49	71	45
3	123	157	121
4	81	136	101
5	98	140	133
6	111	110	149
7	175	132	174
8	173	59	83
9	159	68	59
10	169	74	96
11	132	135	164
12	206	189	78
13	166	155	118
14	224	227	226
15	65	75	72

To confirm the repeatability of developed color palette twenty identical color palettes were made. As it is shown in figure 27 visually these palettes look similar. However, for the industry it is necessary to develop an independent method of control. In colorimetry, color difference value helps to express numerically how different two colors are.

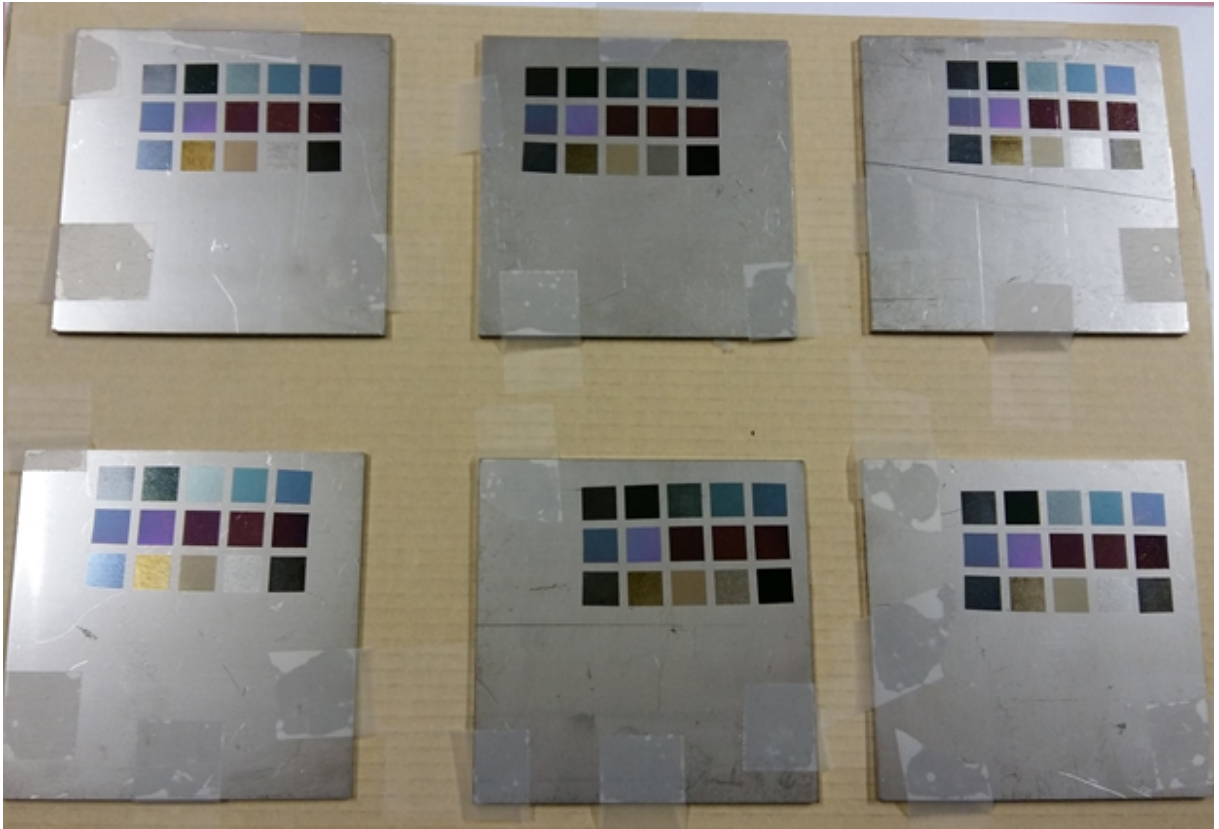


**Figure 27.** Six identical color palettes made with the same parameters of laser processing.

International commission on Illumination developed the standard for the color difference by defining the concept of Delta E. The color difference delta E is the difference between two colors, defined as the Euclidean distance between two points representing these colors in the coordinate systems in one of CIE Euclidean color spaces (either CIE L\*a\*b\* or CIE L\*C\*h\*). Generally, the value of delta E is in range from 0 to 100. Wherein, the correspondence between the value of delta E and visual sensation of human eye can be different, depending on the physiology or illumination conditions. The standard table of connection between perception and delta E is presented below.

*Table 5. Correlation between value of delta E and a human eye perception (X-Rite 2007).*

<b>Delta E</b>	<b>Perception</b>
$\leq 1$	No color difference can be noticed by human eye
1 - 1.5	The difference can be noticed only by perceivable or professional observer
1.5-2	Minimal difference between colors that can be noticed through close study
2-10	Perceptible difference
11-49	Similar colors
100	Opposite colors



To evaluate the color difference in production the value of  $\Delta E = 2$  is usually used (Datacolor official website 2017).

This standard was introduced in 1976 and then was modified twice in 1994 and 2000.  $\Delta E 2000$  avoids some shortcomings of the previous versions so has better tolerance but at the same time it can be considered as the most difficult for calculations. The algorithm of the determination is described in (Sharma, Wu & Dalal 2005, pp. 24-26).

All the calculations were done using MathLab software, with the additional conversion from the CIE RGB coordinates.

Described method is used to prove the repeatability of obtained colors. One of obtained color palettes were chosen as the reference sample. Then, each color of nine other samples was compared with the reference one using the calculator. The value of  $\Delta E$  averaged for all the samples of the same color. The average  $\Delta E$  value of each color square is shown as a graph in figure 28.

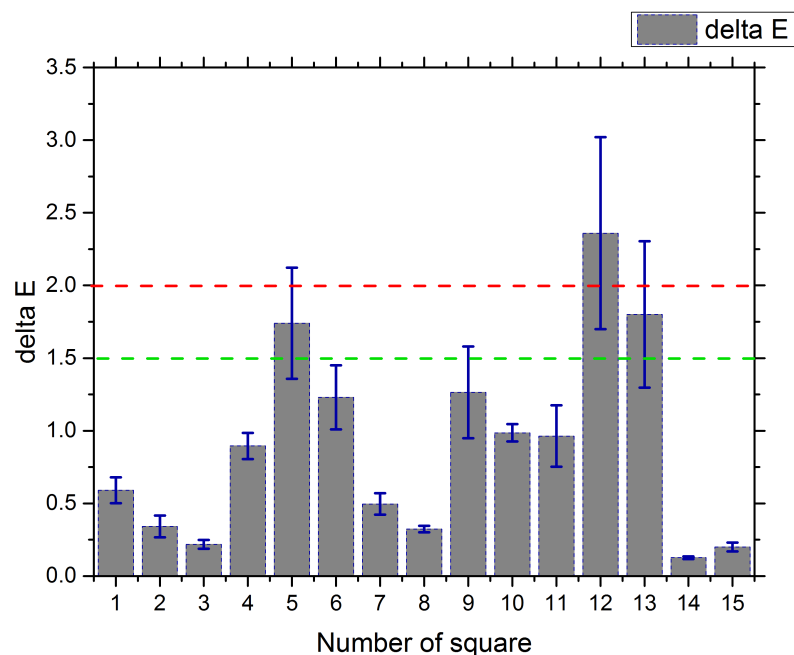


**Figure 28.** The value of  $\Delta E$  for fifteen different colors averaged by ten samples. Green line is the minimal value of  $\Delta E$  which is perceptible for the human eye. Red line is the maximum value acceptable in production.

As it can be concluded from the graph, generally all colors have a good repeatability and can

be used in production. Most color squares (number 1, 2, 3, 7, 8, 14 and 15) have excellent delta E values. Color difference can not be noticed even through close observation by a perceivable observer. Squares number 4, 6, 10 and 11 have rather good values of delta E. Color difference can be noticed only by a professional perceivable observer in good lighting conditions. The delta E value of 9<sup>th</sup> square is satisfactory, but this variation can be accepted for using in production. Samples number 5 and 13 have higher average delta E. Such result can be related to “angle effect” (Ageev et al. 2017b) which appears for some regimes more, than for another. However, these colors still can be included in the color palette, because visually no difference between ten samples was registered. Sample number 12 has the highest delta E and respectively lowest repeatability. The average value of delta E for this square is 2.36 that means that the difference can be perceived by an average observer. Indeed, the color of this square for number of color palettes was noticeably different under the close visual observation. This color can not be proposed to further use, This problem will probably be solved by adjusting the laser processing parameters or by selection of another regime which can provide the similar color.

In conclusion of this section, the complete colorimetric analysis of the color palette was performed. Tests and calculations showed that obtained colors mostly have good uniformity, they are bright and cover almost all spectral regions. Despite the color with the determined colorimetric characteristics can not be produced by this method, the color palette is rather rich for the stainless steel AISI 304. Furthermore, it is possible to extend the number of colors in the palette by development of new regimes of laser irradiation.

The good repeatability and stability of colors was proved by comparison of ten color palettes both visually and using well known in colorimetry concept of color difference, which is based on the juxtaposition of color coordinates of the examined colors. Only one sample showed low repeatability, thus, it needs to be replaced from the final color palette.

## 5.2 Environmental chamber test

Coatings and marks can be applied for the different products and mechanisms that can relate to the different operate conditions, i.e. indoor or outdoor manipulations, high humidity, extreme temperatures etc. At the same time, the mark or coating should withstand all the environmental conditions and do not transform during exploitation of the item. To understand how the applied coating will react to the different atmosphere conditions and environmental changes, it is required to perform the whole examination with determined conditions. To reproduce the necessary

conditions of extremely high or extremely low temperatures or high humidity, environmental chamber tests can be utilized.

In the current work, the environmental tests were performed under the four different operational conditions. The experiment was conducted at the Ioffe Institute, Saint Petersburg. Frequently, the temperature and humidity parameters for the experiment are taken with excess of real values to insure the stability of examined parts for the normal conditions. On the other hand, exposure time in the experiment is 24 hours which is much shorter than real exploitation time. Thus, the experimental conditions have to be chosen with an excess of the actual values of temperature and humidity that are characteristic of operation.

Since the field of implementation of color marking can be wide enough the testing conditions should cover all the possible temperature-humidity range. Thereby, tests was performed at the conditions sown in table 6. It can be said, at proposed parameters the conditions of extremely low temperature with a high percentage of humidity which represents the outdoor work conditions in winter or indoor conditions with decreased temperature (for example commercial refrigerators). Then average temperature with a high humidity that represents the same type of outdoor and indoor conditions closer to the actual production. Then high temperature with a high humidity and extremely high temperature with a high percentage of humidity represent operation conditions related to the use of heating equipment, boilers, welding tools etc., or outdoor works in hot and humidity environment. Thus, the results can give the complete information about the possible area of usage color laser marking in real production conditions.

*Table 6. The environmental chamber conditions.*

<b>Number of test</b>	<b>Temperature, °C</b>	<b>Humidity, %</b>
1	-20	70
2	-40	90
3	40	70
4	100	90

The first test does not show any changes in the colors or material. In figure 29 performed the visual appearance of the color palette after 24 hours in the environmental chamber. Pictures were taken from the different angles. With the optical microscopy analyses was not find any damages or faults in the color oxide films.

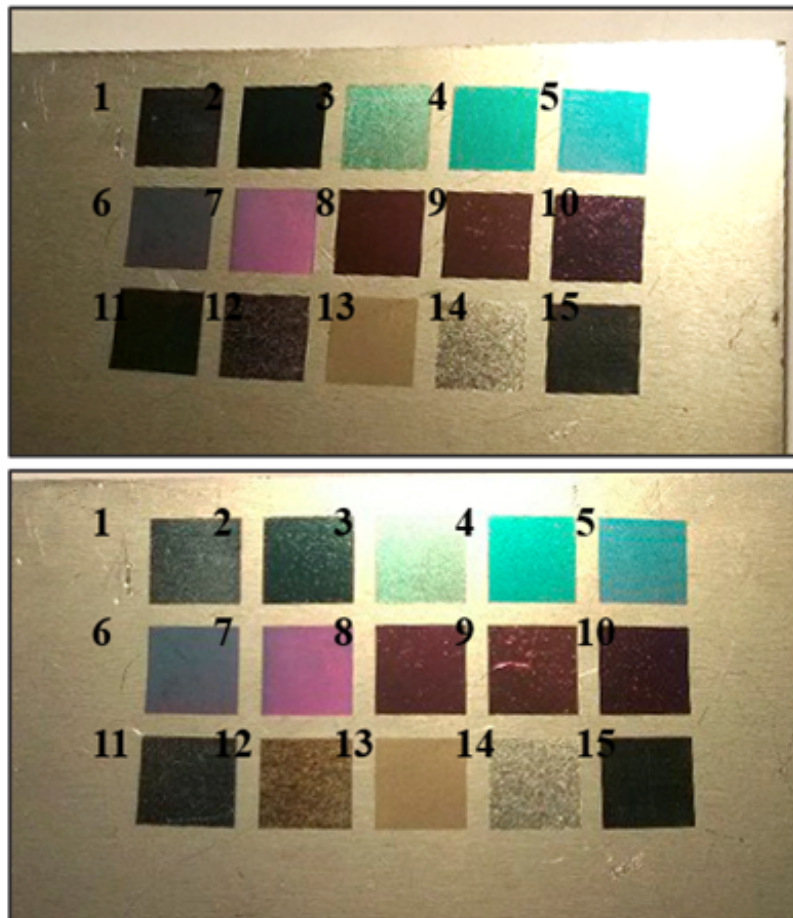


**Figure 29.** The color palette after 24hs exposure in the environmental chamber at  $T = -20\text{ }^{\circ}\text{C}$  with humidity of 70 %.

Next test was related to heavier external conditions with lower temperature and higher humidity. The picture of the color palette after 24 hours at the condition performed in the table 6 is shown in figure 30.



**Figure 30.** The color palette after 24hs exposure in the environmental chamber at  $T = -40\text{ }^{\circ}\text{C}$  with humidity of 90%.

This sample shows several minor changes of the surface after the exposure in the environmental chamber. Pictures of the problematic areas as well as microimages of faults are shown in figure 31. Square number one has one dark stain of about  $400\text{ }\mu\text{m}$  diameter on its surface. Under the closer observation with the optical microscope (figure 31b) this spot is a modified oxide layer with significant damage. The rest of this square does not show any changes. Probably, appearance of the stain is related to the presence of some dirt on the surface or to the impurity in the material. Appearance of this kind of faults has the random character and was noticed only once during the whole experiment.

Sample number five slightly changed color from blue to gray on the periphery of the treated area. Under the microscope this damage looks like appearance of dark areas on the grain boundaries. This effect might be related to the partial oxidation of the sample. A detailed study of sample number five revealed only one damaged area with dimensions of approximately  $1 \times 1.5\text{ mm}$  and this kind of faults was characteristic of only one color, thus, probably related to the regime of laser action.

Sample number ten showed the color degradation on the periphery of the obtained area. Color changed from wine red to yellow, and the size of this area was about  $1 \times 0.5\text{ mm}$ . Microscopic analysis demonstrated the damaged area where the oxide film has been etched. Thereat, the structure was not destroyed. This fault can appear due to a high humidity and probably these areas will enlarge with the increase of the exposure time. This kind of etched microspots were observed in the other samples, but they can not be distinguished by visual observation as they

have the size about 1-3  $\mu\text{m}$  and mainly located near the periphery.

At the same time, no faults of initial material were noticed neither by visual observations nor the microscopy. Thus, it can be concluded that generally this color laser marks can stand the conditions of low temperatures and high humidity. However, color palette is recommended to be slightly modified for these purposes.

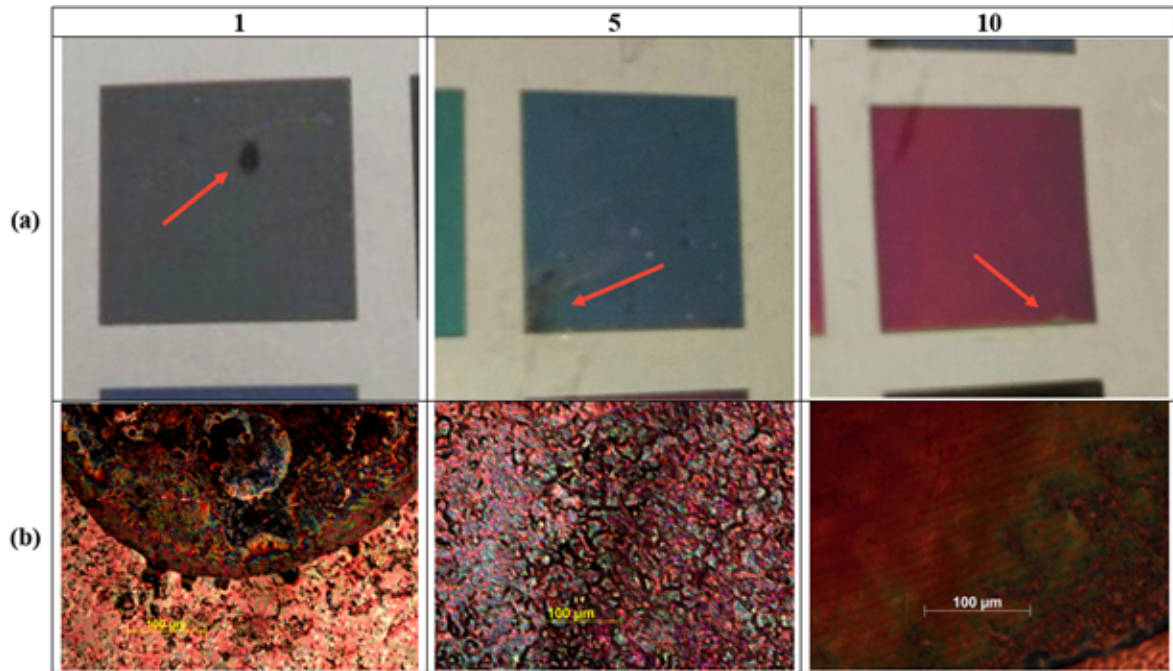


**Figure 31.** Faults of colors after 24hs exposure in the environmental chamber at  $T = -40\text{ }^{\circ}\text{C}$  with humidity of 90%: photos - a), microimages - b).

This sample was placed to the environmental chamber at high temperature and humidity. After exposure during 24 hours the palette does not receive any significant faults (figure 32). No changes in colors or metal surface was noticed.



**Figure 32.** The color palette after 24hs exposure in the environmental chamber at  $T=40\text{ }^{\circ}\text{C}$  with humidity of 70%.

However, after detail examination the damage of one square was detected. One corner of square number 4 has a stain with size of approximately 1x2 mm which is visible at a certain angle (figure 33a). Under the microscope this stain is the partial darkening of the oxide film (figure 33b). This kind of damage was noticed previously in the square number 5 after the second test. As well as there, it might be due to laser processing parameters.

In general, the palette proved to be stable to the rather high temperature conditions but some colors should be tested more detailed and need to be replaced if faults appear.

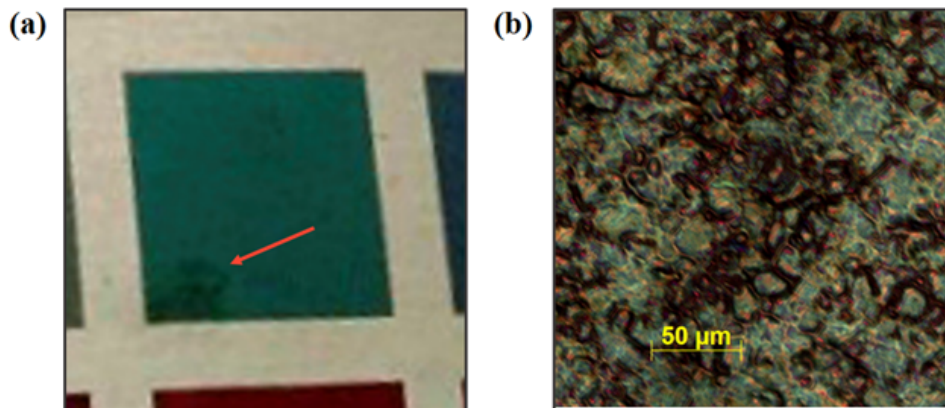


**Figure 33.** Fault with 4th color after 24hs exposure in the environmental chamber at  $T=40\text{ }^{\circ}\text{C}$  with humidity of 70%: photos (a), microimages (b).

Last sample was tested under extremely rough conditions explained in the table 6. The sample got a number of lacks, i.e. dark spots and stains on the surface of metal itself as well as on the

colors, that can be well seen in the figure 34.

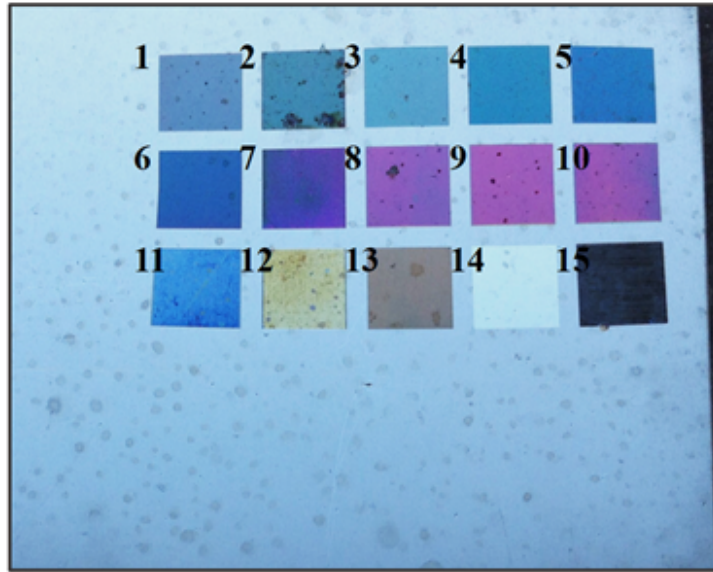


**Figure 34.** The color palette after 24hs exposure in the environmental chamber at  $T=100\text{ }^{\circ}\text{C}$  with humidity of 90%.

The most visible faults are shown in figure 35a. Almost all color squares were damaged more or less in form of dark stains as it shown for squares number 2 and 8. The size of these stains varies from  $500\text{ }\mu\text{m}$  up to  $3\text{ mm}$  and does not depend on the laser processing parameters thus on the color. Under the detailed examination with the optical microscope, these stains are complete destruction of the oxide layer (figure 35). Probably due to extremely high humidity, water condensates on the surface in small drops and which evaporates on metal because of high temperature in the chamber. The recoil vapors cause the degradation and the strike destruction of the thin oxide layer.

On the other hand, untreated surface showed bad sustainability to this kind of environmental conditions as well. On the entire surface of the untreated steel, there are dark spots with characteristic dimensions from about  $0.5$  to  $2\text{ mm}$ . When observing the surface through an optical microscope, dark areas were noticed. Darkening might be associated with the oxidation (rusting) of certain areas of the surface. These spots can be related to the condensation and subsequent evaporation of water on the metal that result on the partial oxidation.



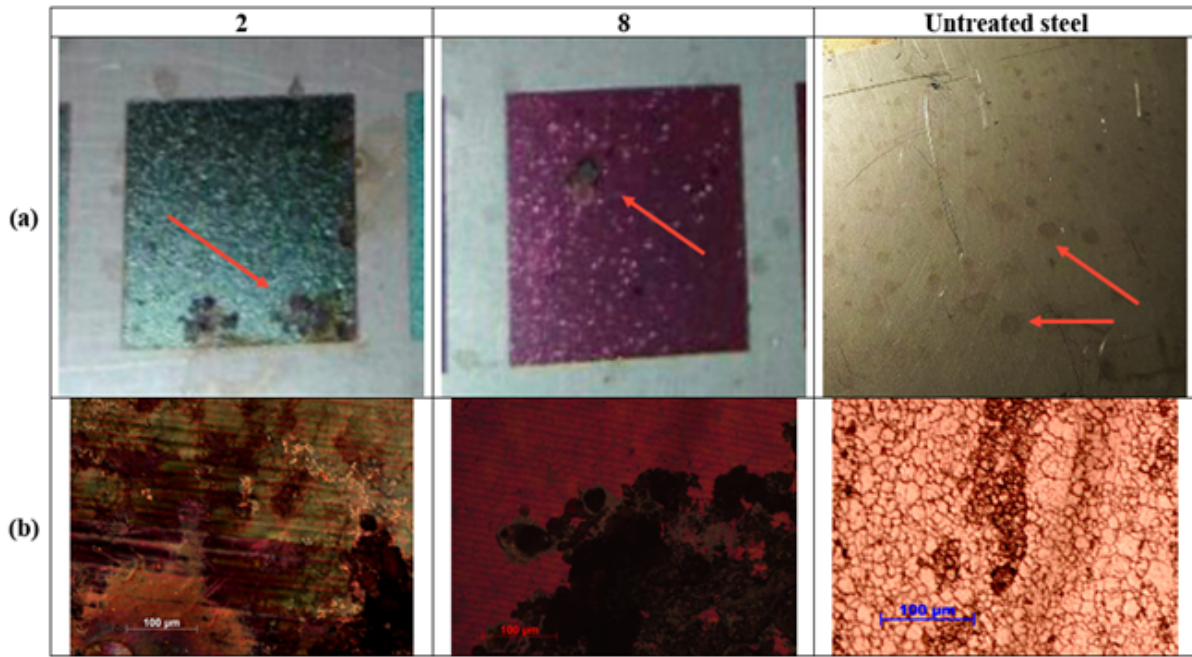


**Figure 35.** Fault of colors after 24hs exposure in the environmental chamber at  $T= 100\text{ }^{\circ}\text{C}$  with humidity of 90%: photos - a, microimages - b.

Thus, the last test showed the impossibility of applying color laser marking in the extremely rough conditions of elevated temperature and humidity. However, if there is sufficient air circulation in the working place, the risk of damage to the color coating can be reduced to insignificant values.

All the described color faults are associated with the appearance of bounded damaged zones or clusters with a changed color. This indicates that the oxide film is uneven in structure and the damage appears in the weakest areas. This may be due to the unevenness of the chemical composition of the basic material, as well as to the laser marking technology, which is associated with the continuous reformation of the relief and, accordingly, with the formation of a non-uniform thickness and structure of the oxide film. This unevenness can be observed on microimages 20 of samples in the form of clusters of different colors, which are respectively indicators of a different thickness of the film.

In general, the tests showed good results proving the stability of color laser marking to various environmental conditions, including conditions of low and high temperatures at high humidity. The color palette can be refined taking into account the minor faults found during the tests with the environmental chamber.

### 5.3 Mechanical resistance

Mechanical resistance of a material frequently depends on its hardness. In case of covers and films, indentation hardness of the cover much less than hardness of a substrate. There are several different techniques of determination the indentation hardness, including Vickers, Brinell , Knoop, Rockwell tests etc (Chandler 1999). For foils, films and other thin materials usually it is required to find microhardness, thus, microindantation Vickers and Knoop tests with a light load can be used (Jönsson & Hogmark 1984, Osten 2016).

In this work Vickers microhardness test was performed for obtained an untreated material. The test was conducted by means of International Laboratory “Laser Micro and nanotechnologies” in ITMO University, Saint Petersburg.

According to the methodology of Vickers test, hardness can be calculated (Chandler 1999, p. 42):

$$H = 0.189F_n/d_i^2 \quad (17)$$

Where  $F_n$  is normal load,  $d_i$  is the mean of diagonals left by indenter

Determined values of hardness as well as microimages of indent are shown in Table 7.

*Table 7. Microhardness of obtained samples.*

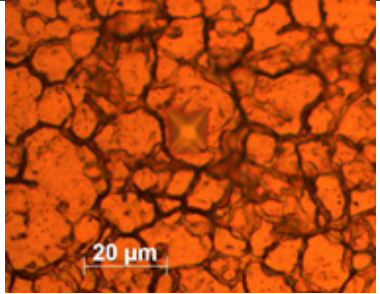
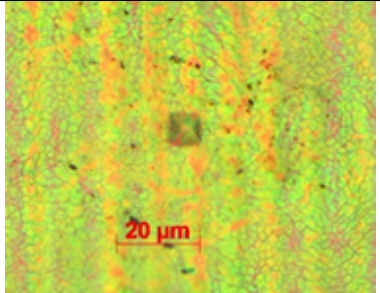
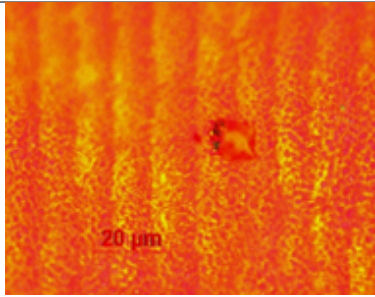
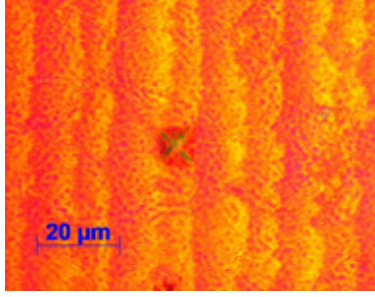
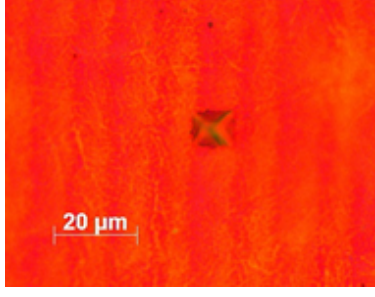
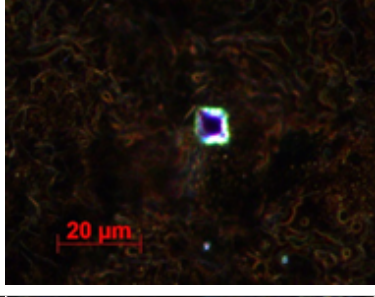
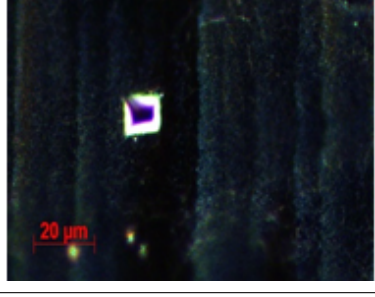
Number of sample	Hardness H, HV	Microimage of the indent
Untreated steel	180	
2	136	

Table 7 continues. Microhardness of obtained samples.

Number of sample	Hardness H, HV	Microimage of the indent
8	133	
9	129	
10	135	
11	167	
15	128	

For most samples, the hardness was much less than that of untreated steel. A volume density of oxide obviously much lower than a density of metal, thus oxide films have lower indentation hardness.

Sample number 11 had highest hardness among the laser treated colors. Probably it is related to relatively small overlap and lower power density than other colors, thus, the oxide film which is grown during laser processing is thinner than for other regimes. For such thick films the substrate might make a significant contribution to the measurement. Nevertheless, hardness of obtained surface is rather high that can approve the wear resistance of the covering to the external mechanical impact.

#### 5.4 Chemical resistance

In different field of productions parts can be in contact with different chemical agents. This fact make one more demand to the technology: marks must stand the interaction with the chemicals which are used in the specific case.

In industry, there are a lot of fields there might occur the contact of mark with the different chemical solutions. For various properties the solutions of acids, salts, surfactant, alcohols or other agents can be utilized. Therefore, in the current the analyze of chemical resistance is also performed.

Sulfuric acid is widely used nowadays in industry. It have such applications as paper production, iron and steel pickling, production of agricultural agents, water treatment etc. Thus, first test was carried out with the use of 3% Sulfuric acid solution. Sample was placed into solution for 48 hours. After 24 hours colors became less saturated, some of them had changed to another (square 10 changes partially from red to green). The final result is performed in figure 36.

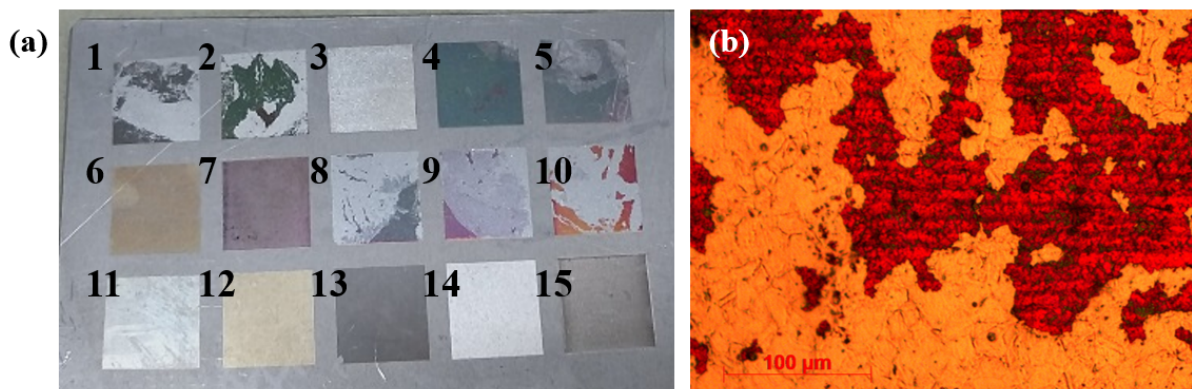
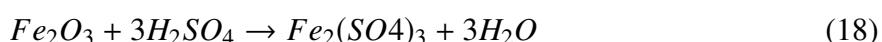


**Figure 36.** Color palette after 48 hours in 3% sulfuric acid: photo (a), microimage of 9<sup>th</sup> square (b).

How it can be noticed from the picture, colors were erased partially or completely from the

surface. The process of chemical etching in sulfuric acid occurred according to reaction:



It should be mentioned that during rinsing by pure water, the film was being removed in a form of large pieces of approximately 2-3 mm in dimensions.

As  $Fe_2(SO_4)_3$  is highly soluble in water, no additional products of the chemical reaction was observed. Concentration of the solution is only 3% and in actual production this value can be even higher. Thus, colors can not stand long interaction with an acidic environment.

In production tools and parts are often exposed to caustic soda solutions of varying concentrations. The first test shows how the color marking is resistant to interaction with alkali. For this, the sample of the final palette was placed in a 10% solution of NaOH for 48 hours. After the exposure sample was rinsed with pure water. The result is shown in the following figure.

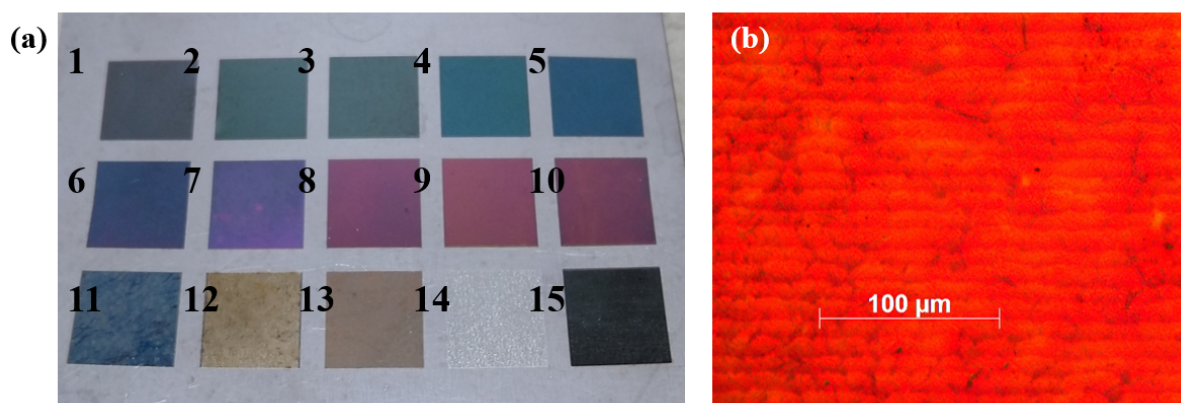


**Figure 37.** Color palette after 48 hours in 10% NaOH: photo (a), microimage of 9<sup>th</sup> square (b).

No significant changes were mentioned both after 24 and 48 hours. For manufacturing purposes 3-5% NaOH solutions are used that is much lower than the experimental concentration. It can be concluded that produced color covering is rather stable in an alkaline.

Alcohols are usually used in chemical and fuel industry, food industry, medicine, cosmetics and many other areas. Next test was performed with the use of technical ethanol (98%). Sample was kept in solution also for 48 hours. In figure 38 the result of the experiment is performed.

Colors did not change and both visual and microscopic observations did not show any faults.

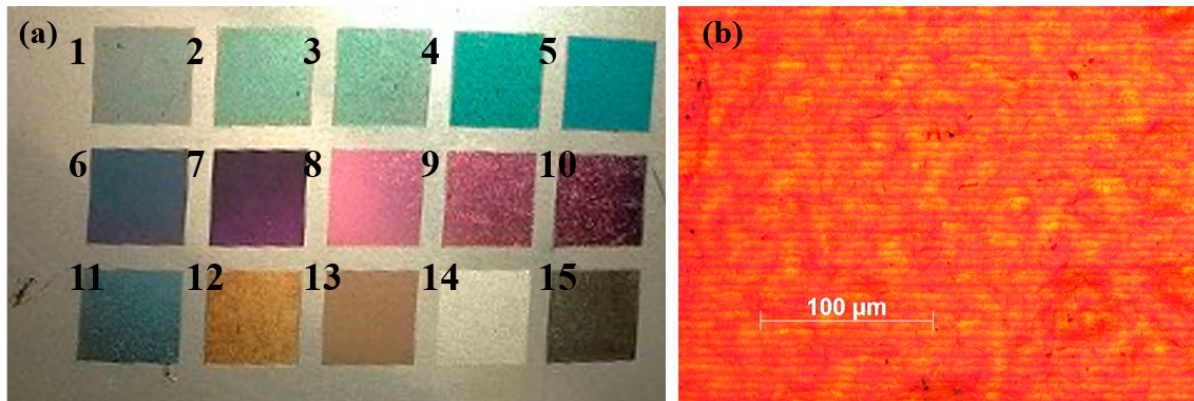


**Figure 38.** Color palette after 48 hours in 99% ethanol: photo (a), microimage of 9<sup>th</sup> square (b).

Next test was carried out with standard industrial surfactant (New ultrasil 69) which has 13 pH and contains 1.5% phosphorus (Kelley Supply, Inc. official website 2017). Surfactants or surface active agents it is a class of different compounds which are used for cleaning, dispersing or wetting surface. It is the main component of detergents, soaps, anti-fogs, emulsions, cosmetics etc. The result of 48 hours exposure in surface active agent is shown in figure 39. Colors survived the effect of the cleaning agent and no faults were noticed.

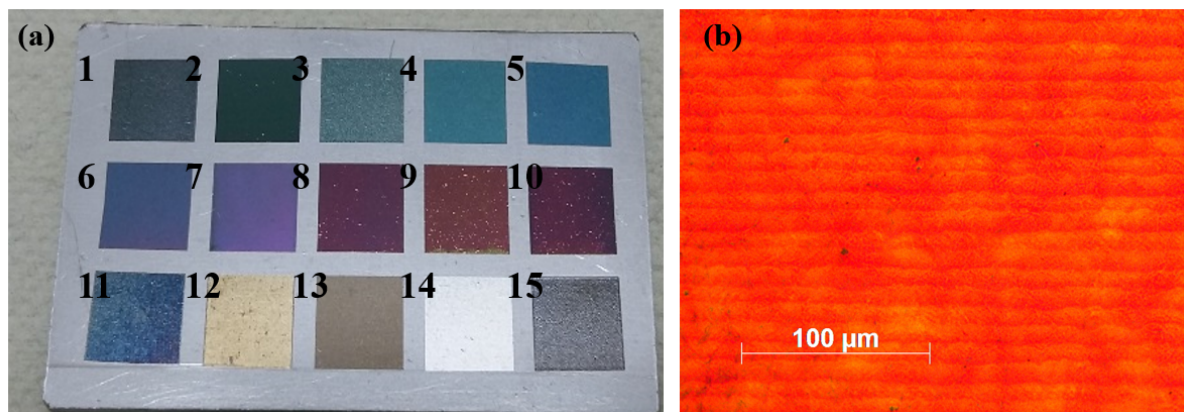


**Figure 39.** Color palette after 48 hours in Ultrasil New 69 surfactant: photo (a), microimage of 9<sup>th</sup> square (b).

Last test was conducted with NaCl 10% water solution. Sample placed into the solution for 24 hours and visual appearance of it is shown in figure. Some colors have withstood the saline solution, but most of them have been spoiled. The entire sample began to rust. The largest

damage was received in samples number 1, 2 and 15. It can be clearly seen from the photograph that rusting begins on the periphery of each colored square and extends further to the untreated material. It can be concluded that oxidation is associated with thermal damage to the natural protective layer of stainless steel. On squares 2 and 15 it can be seen that the oxide film broke up partially and split off from the surface.

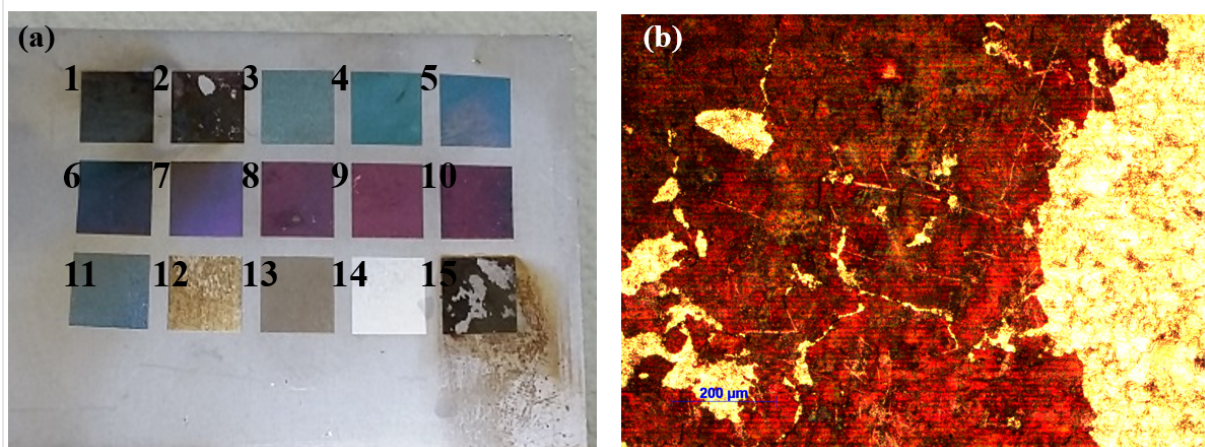


**Figure 40.** Color palette after 24 hours in 10% NaCl: photo (a), microimage of 2<sup>nd</sup> square (b).

Therefore, it was proved that color laser marking is suitable for close work with some of chemicals such as alcohols, surfactants and caustic. soda. However, marks can be damaged by long interaction with acidic solutions and salts. Thus, it can be recommended to avoid industrial fields with a presence of acidic and salty environment.

## 6 RESULTS AND CONCLUSION

In the presented thesis work the issue of the possibility of using color laser marking technology in production and the introduction of technology into various areas of actual industry was discussed in detail. At the same time, the most important aim was to check the reliability of the marking when applying it in various possible operating conditions. To achieve this goal, it was necessary to consider a number of objectives formulated at the very beginning of the this project, which were successfully implemented. The physico-mechanical and chemical properties of the obtained coating were investigated from the point of view of their resistance to external action. The question of the repeatability of the color palette, also developed in the current work, was also taken into account.

During the preparatory stage, investigations of various research groups related to the topic of the thesis was studied. A comparison with traditional methods of applying color coatings to metals is made. The main features of laser deposition technology are revealed, advantages and possible limitations of use are formulated. Laser marking is characterized by high quality of the applied image, the ability to apply several colors at once in the same operation circle, high process performance and the lack of additional consumables. In addition, a significant advantage is the absence of any additional dyes or chemicals, which increases its environmental friendliness. Also, the main principles of interaction of radiation with matter and possible technological solutions for color laser marking have been discussed. It is shown that fiber infrared lasers with nanosecond pulse duration are the most suitable instrument for the industrial introduction.

The next stage of the work consisted in the preparation and adaptation the experimental setup based on a nanosecond fiber ytterbium laser for the color marking of metals. First of all, a review of the parameters of the used equipment and an analysis of the individual parts of the installation was conducted. During the preparation for the work, the scanning system was calibrated and the characteristics of the laser beam in focus point were analyzed. The laser spot distribution on the surface was measured in order to find right value of power density. A number of preliminary tests were performed to determine the parametric window when working with AISI 304 stainless steel for further work. The dependence of the obtained colors on such parameters of laser radiation as radiation power, repetition rate, pulse duration, and scanning speed are shown in the work. At the output was developed a palette for stainless steel AISI 304, consisting of 15 different colors,



which was studied at subsequent stages.

First of all, the visual appearance of the oxide layer, its structure and relief was investigated. With the help of optical microscopy revealed that the structure of the oxide film for most colors is non-uniform and the films consist of regions of different thickness, clearly distinguishable by the characteristic color. It is concluded that the resulting color is a superposition of individual contributions from the microregions of different colors on the surface. The surface relief is also irregular, which showed both SEM and AFM analysis. Raman scattering spectroscopy was used to find the composition of the obtained oxide films. Peak analysis showed that the film consists of two main components:  $Fe_2O_3$  and  $FeCr_3O_4$ . These measurements are confirmed by data obtained earlier by other researchers.

The standardization of colors was carried out in accordance with the standards of the International commission on Illumination. With the help of spectrophotometric measurements, reflection spectra of each color were obtained. The light coordinates in the CIE RGB color space are calculated. The resulting colors have high contrast and belong to the different color tones. The repeatability of the result is shown by calculating the value of delta E. In general, the color palette has a high repeatability, but certain colors are recommended to be replaced, since they do not meet the minimum requirements of delta E value for industry.

The stability of color laser marking to the effect of various weather conditions reproduced by means of a climatic chamber is shown. The behavior of color palettes under conditions of high and extremely high humidity at high and low temperatures was considered. The test showed that the color palette has a high resistance to low temperature conditions. The sample successfully passed the test for a temperature of  $-20\text{ }^{\circ}\text{C}$  and a humidity of 70%. When the temperature is lowered to  $-40\text{ }^{\circ}\text{C}$  and the humidity rises to 90%, a prolonged exposure results in a slight modification of several colors, which were recommended to be replaced by more stable ones. At high temperatures of  $40\text{ }^{\circ}\text{C}$  and a humidity of 70%, some colors also showed unsatisfactory results, but in general the palette showed good resistance to such an effect. At extremely high temperatures and high humidity ( $100\text{ }^{\circ}\text{C}$ , 90%), partial destruction of some colors occurred, in addition, the surface of the untreated metal also suffered damage. This method of marking is not recommended for prolonged use of the part in conditions of high humidity and temperature. In general, color marking can be used for both indoor and outdoor applications.

The mechanical stability of the color palette was shown by finding the value of Vickers hardness before and after laser treatment, using a microhardness tester equipped with a diamond pyramid. The test showed that although the hardness of the samples after treatment is on average 25% lower than the hardness of the substrate material. Despite this, the hardness of the coatings is quite high, due to which a high mechanical stability of the color marking to external influences is ensured. Moreover, since the color is obtained not by applying an additional coating, but by modifying the surface itself, the adhesion of such labels is much higher than of conventional methods.

At the final stage, the stability of the color palette against the effects of various chemical reagents was checked. After longtime exposure of the palettes in a NaOH 10% solution, as well as in the technical ethanol (99%) and in industrial cleaner (Ultrasil New 69), no changes in the color or structure of the oxide layer were detected. Thus, color laser marking can be used for parts that involve interaction with the chemicals listed above. When exposed to 48 hours 3% sulfuric acid solution, the colors were completely damaged. Thus, exposure to acid media can damage the marking during the operation of the part. In such cases, it is recommended to use other marking methods or laser engraving to ensure label stability. 10% solution of table salt (NaCl) when interacting with the color mark initiates rusting of the material, which is unacceptable in production. Apparently, this is due to the fact that the laser action damages the natural protective layer of stainless steel. Color marking and engraving are not recommended for use in production areas associated with the use of salts or acidic environment.

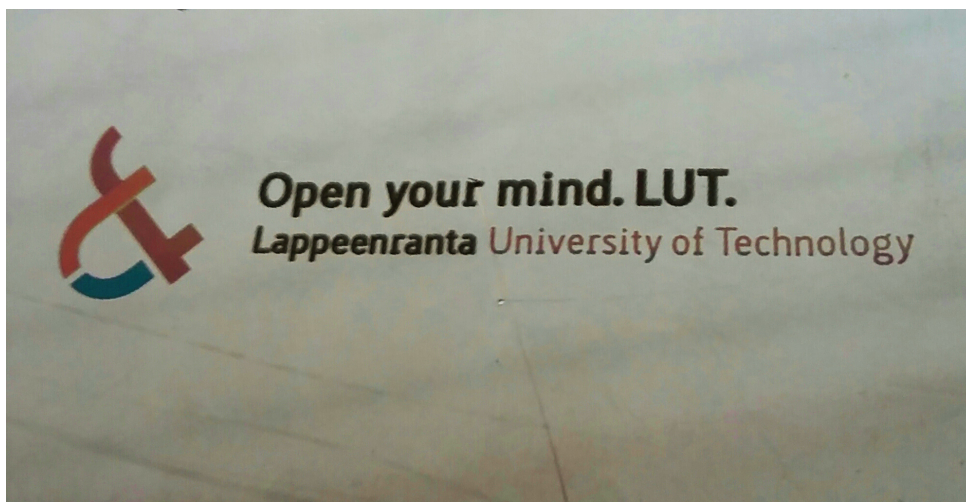


**Figure 41.** An example of color mark on stainless steel (LUT logo).

In conclusion, it can be said that color laser marking is a promising direction of industry and

can be used in various fields of production. In the figure 41 an example of produced color mark is shown. The use of a fiber laser can significantly simplify the introduction into existing production lines. However, this type of marking is not suitable for identifying products intended for use in conjunction with acid and salt media. It is also worthwhile to avoid the use of such labels under extremely high temperatures at a sufficiently high humidity. It should be noted that in this case it is a question of marking on products made of stainless steel. For other materials, such as titanium or tungsten carbide, the color coatings may have a higher physico-chemical stability.

## 7 SCOPE OF FUTURE STUDY

In this paper, the answers to all research questions posed in the introduction were found and studied in detail. The main principle of the technology of color laser marking is considered, the properties of the obtained coatings are tested, the colors are checked for repeatability and wear resistance to physical, mechanical and chemical influence. However, there are also a number of other tasks that are not relevant to the subject of this work, which are necessary for introducing the technology to the market.

One of the most promising directions of the research development is the extension of the color palette for AISI 304 stainless steel and increased productivity of marking. In spite of the fact that in this thesis the obtained color palette is rather wide and includes all the basic colors, for successful application of the technology it is necessary to develop a wider palette, including at least 30 different colors. For this, it is proposed to use processing regimes with different pulse durations, and also to vary over a wider range of overlap values  $L_x$  and  $L_y$ . To improve productivity, it is possible to use more powerful lasers, as well as modes with higher frequencies.

The second important area for further research is the increasing the material base for technology. It is known that color laser marking is possible for various oxidizable metals, for example, different grades of steel, titanium, chromium, brass, tungsten carbide, etc. Since the technology is associated with a physico-chemical modification of the surface, for each material the color palette will be different. Thus, it is necessary to search for parametric windows for each material and to develop color palettes also for them.

Another important aspect of the study is the high dependence of the obtained colors on the focusing mode, that is, the sensitivity of the installation to the position of the object being marked. Since in production conditions it is not always possible to provide high precision positioning of the part, color marking can vary significantly due to the different size of the laser spot on the surface. For this, a feedback system can be built into the laser system, which allows tracking the position of the part and is able to correct the conditions of the action in real time to ensure the same temperature distribution over the surface during processing.

**REFERENCES**

- Adams, D. P., Hodges, V., Hirschfeld, D., Rodriguez, M. A., McDonald, J. and Kotula, P. G. 2013. Nanosecond pulsed laser irradiation of stainless steel 304L: Oxide growth and effects on underlying metal. *Surface and coatings technology*, 222. Pp. 1–8.
- Ageev, E., Andreeva, Y. M., Karlagina, Y. Y., Kolobov, Y. R., Manokhin, S., Odintsova, G., Slobodov, A. and Veiko, V. 2017a. Composition analysis of oxide films formed on titanium surface under pulsed laser action by method of chemical thermodynamics. *Laser Physics*, 27: 4. Pp. 1-9.
- Ageev, E., Andreeva, Y., Brunkov, P., Karlagina, Y., Odintsova, G., DV, P., Pavlov, S., Romanov, V. and Yatsuk, R. 2017b. Influence of light incident angle on reflectance spectra of metals processed by color laser marking technology. *Optical and Quantum Electronics*, 49: 50. Pp. 1-7.
- Amara, E., Haïd, F. and Noukaz, A. 2015. Experimental investigations on fiber laser color marking of steels. *Applied Surface Science*, 351. Pp. 1–12.
- Baddoo, N. R. and Burgan, B. 2001. *Structural design of stainless steel*. Berkshire, UK: Steel Construction Institute London. 320 p.
- Birks, N., Meier, G. H. and Pettit, F. S. 2006. *Introduction to the high temperature oxidation of metals*. 2nd edition. Cambridge, UK: Cambridge University Press. 336 p.
- Blawert, C., Dietzel, W., Ghali, E. and Song, G. 2006. Anodizing treatments for magnesium alloys and their effect on corrosion resistance in various environments. *Advanced Engineering Materials*, 8: 6. Pp. 511–533.
- Blower, R. and Evans, T. 1974. Introducing coloured stainless steel. *Sheet Metal Industry*, 51: 5. Pp. 230–234.
- Bostroem, A., Bekolay, T. and Staneva, V. 2016. Programming with Python: Figures. *Procedia Computer Science*, 88.
- Bouzakis, K.-D. and Michailidis, N. 2014. Physical vapor deposition (PVD), *CIRP Encyclopedia of Production Engineering*. Pp. 939–946.

Burns, R. M. and Bradley, W. W. 1967. Protective coatings for metals. American Chemical Society: 163.

Chandler, H. Introduction to hardness testing, Mechanical testing and evaluation. 2nd Edition. Cleveland, USA: ASM International, 1999. 194 p.

Chu, S. J., Devigus, A. and Mielezsk, A. J. 2004. Fundamentals of color: shade matching and communication in esthetic dentistry. New York, USA: Quintessence Publishing Company. 168 p.

Cui, Ch., Hu, J., Liu, Yu., Gao, K. and Guo, Z. 2008. Morphological and structural characterizations of different oxides formed on the stainless steel by Nd: YAG pulsed laser irradiation. Applied Surface Science, 254. Pp. 6537–6542.

Datacolor official website. Support webpage [web document]. Updated 2008 [Referred 31.3.2017]. Color differences and tolerances commercial color acceptability. Available in PDF-file: <http://industrial.datacolor.com/support/articles/>

Dusser, B., Sagan, Z., Soder, H., Faure, N., Colombier, J.-P., Jourlin, M. and Audouard, E. 2010. Controlled nanostructures formation by ultra fast laser pulses for color marking. Optics express, 18: 3. Pp. 2913–2924.

Gardiner, D. J., Littleton, C. J., Thomas, K. M. and Strafford, K. N. 1987. Distribution and characterization of high temperature air corrosion products on iron-chromium alloys by Raman microscopy. Oxidation of metals, 27: 1. Pp. 57–72.

Gorbunova, E. V., Chertov, A. N., Peretyagin, V. S., Lastovskaia, E. A., & Korotaev, V. V. 2015. The area of applicability of apparatus for analyzing the spectral characteristics of reflection, albedo and color parameters of flat objects. SPIE OPTO. International Society for Optics and Photonics, 93690.

IPG Photonics Corp. 2017. YLPM series pulsed ytterbium fiber lasers user's guide. [web document]. Updated 3.02. 2017 [Referred 31.3.2017]. Available at: <http://http://www.ipgphotonics.com/en/products/lasers/nanosecond-fiber-lasers>

Jervis, T., Williamson, D., Hirvonen, J.-P. and Zocco, T. 1990. Characterization of the surface oxide formed by excimer laser surface processing of aisi 304 stainless steel. Materials Letters, 9: 10. Pp. 379–383.

Jönsson, B. and Hogmark, S. 1984. Hardness measurements of thin films. *Thin solid films*, 114: 3. Pp. 257–269.

Junqueira, R. M. R. and de Oliveira Loureiro, C. R. (2014). Electrochemical coloration of stainless steel as an alternative for architectural coatings. *Blucher Chemistry Proceedings*, 2: 3. Pp. 37–48.

Kelley Supply, Inc. official website [web document]. Updated December 2017 [Referred 31.3.2017]. Ultrasil 67 and ultrasil 69 new. Available in PDF-file: [http://www.kelleyssupply.com/customer/kelsup/customerpages/specpages/chemicals/ecolab/ecolab\\_product\\_spec\\_sheets/52151\\_Ultrasil\\_67.pdf](http://www.kelleyssupply.com/customer/kelsup/customerpages/specpages/chemicals/ecolab/ecolab_product_spec_sheets/52151_Ultrasil_67.pdf)

Koenderink, J. J. 2010. *Color for the Sciences*. Boston, USA: The MIT Press. 760 p.

Lawrence, S. K., Adams, D. P., Bahr, D. F. and Moody, N. R. 2013. Mechanical and electromechanical behavior of oxide coatings grown on stainless steel 304l by nanosecond pulsed laser irradiation. *Surface and Coatings Technology*, 235. Pp. 860–866.

Li, Z., Zheng, H., Teh, K., Liu, Y., Lim, G., Seng, H. and Yakovlev, N. 2009 Analysis of oxide formation induced by UV laser coloration of stainless steel. *Applied Surface Science*, 256: 5. Pp. 1582–1588.

Luo, F., Ong, W., Guan, Y., Li, F., Sun, S., Lim, G. and Hong, M. 2015. Study of micro/nanostructures formed by a nanosecond laser in gaseous environments for stainless steel surface coloring. *Applied Surface Science*, 328. Pp. 405–409.

Microscan Systems, Inc. 2017. *Direct Part Marking Methods*. [web document]. Updated 2.3.2017 [Referred 8.4.2017]. Available at: <http://www.microscan.com/en-us/resources/know-your-tech/direct-part-marking-methods>

Misev, T. V. and Van der Linde, R. 1998. Powder coatings technology: new developments at the turn of the century. *Progress in Organic Coatings*, 34: 1. Pp. 160–168.

Ocean Optics Inc. 2016. *Chemusb4 spectrometers user guide*. [web document]. Updated 1.01.2016 [Referred 9.4.2017]. Available: <https://oceanoptics.com/product/chemusb4-spectrometers/>

- Ogura, K., Sakurai, K., Uehara, S. 1994. Room temperature coloration of stainless steel by alternating potential pulse method. *Journal of Electrochemical Society*, 141. Pp 648-651.
- Osten, W. 2016. *Optical inspection of Microsystems*. July 20, 2006, New York, USA: CRC Press. 71 p.
- Pat.EP2834034A1. 2015. A method and a system for color marking of metals. Wroclawskie Centrum Badan EIT Sp (Antonczak, A., Kocon, D., Nowak, M., Kozol, P., Kaczmarek, P., Wa, Z, A. and Abramski, K.). Appl. EP20130724023, 2012-04-05. Publ. 2015-02-11.
- Pat. US9205697B2. 2014. Method For Color Marking Metallic Surfaces. Ferro Corp (Ashtiani, M., Kamal, E., DA, D., Taylor, E., Kamal, K. and Kamal, Y.). Appl. US 14/145163, 2013-12-31. Publ. 2014-12-4.
- Pat. US6238847B1. 2001. Laser marking method and apparatus. Ferro Corp (Axtell III, Enos Ayres and Kapp, David C and Knell, Timothy A and Novotny, Miroslav and Sakoske, George Emil). Appl. US08951411, 1997-10-16. Publ. 2001-05-29.
- Pat. US 4869789A. 1989. Method for the preparation of decorative coating on metals. Technische Hochschule Karl-Marx-Stadt (Kurze, P., Krysmann, W., Berger, M., Rabending, K., Schreckenbach, J., Schwarz, T. and Hartmann, K.-H.). Appl. US07151363, 1987-02-02. Publ. 1989-09-26.
- Panjan, M., Gunde, M. K., Panjan, P. and Cekada, M. 2014. Designing the color of alumin hard coating through interference effect. *Surface and Coatings Technology*, 254. Pp. 65–72.
- Sharma, A. 2004. *Understanding color management*. New York, USA: Thomson & Delmar Learning. 362 p.
- Sharma, G., Wu, W. and Dalal, E. N. 2005. The CIEDe color-difference formula: Implementation notes, supplementary test data, and mathematical observations. *Color Research & Application*, 30:1. Pp. 21–30.
- Shiner, B. 2016. Fiber lasers continue to gain market share in material processing applications. *Manufacturing Engineering*, 156: 2. Pp. 79–85.
- Thibeau, R. J., Brown, C. W. and Heidersbach, R. H. 1978. Raman spectra of possible corrosion products of iron. *Applied Spectroscopy*, 32: 6. Pp. 532–535.



Veiko, V., Odintsova, G., Ageev, E., Karlagina, Y., Loginov, A., Skuratova, A. and Gorbunova, E. 2014. Controlled oxide films formation by nanosecond laser pulses for color marking. *Optics express*, 22: 20. Pp. 24342–24347.

Veiko, V., Odintsova, G., Gorbunova, E., Ageev, E., Shimko, A., Karlagina, Y. and Andreeva, Y. 2016. Development of complete color palette based on spectrophotometric measurements of steel oxidation results for enhancement of color laser marking technology. *Materials & Design*, 89. Pp. 684–688.

X-Rite. 2007. Corporate Headquarters. [web document]. Updated 2007 [Referred 26.4.2017]. A guide to understanding color communication. Available in PDF-file: [http://tqmsystems.nl/uploads/Understand\\_Color\\_en.pdf](http://tqmsystems.nl/uploads/Understand_Color_en.pdf)